Astron. Astrophys. 137, 307–326 (1984)

ASTRONOMY AND ASTROPHYSICS

Observations of Nova Muscae 1983 from 1200 Å–10 μm during its early decline stage*

J. Krautter[1], K. Beuermann[2], C. Leitherer[3], E. Oliva[4], A. F. M. Moorwood[4], E. Deul[5], W. Wargau[6,], G. Klare[3], L. Kohoutek[7], J. van Paradijs[8], and B. Wolf[3]**

[1] Max-Planck-Institut für extraterrestrische Physik, D-8046 Garching bei München, Federal Republic of Germany
[2] Astronomisches Institut der TU Berlin, Ernst-Reuter-Platz 7, D-1000 Berlin 10,
[3] Landessternwarte Königstuhl, D-6900 Heidelberg, Federal Republic of Germany
[4] European Southern Observatory, Karl-Schwarzschild-Strasse 2, D-8046 Garching bei München, Federal Republic of Germany
[5] Sterrewacht Leiden, 2300 RA Leiden, The Netherlands
[6] Dr. Remeis-Sternwarte, Sternwartstrasse 7, D-8600 Bamberg, Federal Republic of Germany
[7] Hamburger Sternwarte, Gojensbergweg 112, D-2050 Hamburg 80, Federal Republic of Germany
[8] Astronomical Institute "Anton Pannekoek", University of Amsterdam, Roeterstraat 15, 1018 WB Amsterdam, The Netherlands

Received January 30, accepted March 6, 1984

Summary. Observations of Nova Muscae 1983 over a wide spectral range from 1200 Å to 10 μm in the time interval January 21, 1983 to March 4, 1983 are presented. Two evolutionary phases were covered: diffuse enhanced and Orion-phase. Spectroscopic observations were carried out in the visual spectral range at medium and high resolution, in the IR range at low resolution, and in the UV range at low and high resolution with the IUE. Broad band photometry was carried out in both the visual (*UBV*, Walraven) and IR (*JHKLMN*) spectral ranges.

It is shown that Nova Mus was discovered several days (3–4) after outburst. A maximum brightness $V_{max} \approx 7$ mag, a lifetime $t_3 \approx 40$ days, and an absolute visual magnitude $M_{V_{max}} = -7.75$ were determined. Hence, Nova Mus 83 can be classified as a moderately fast nova. The distance modulus together with the interstellar extinction $E_{B-V} = 0.45$ (derived from the interstellar 2200 Å feature in the UV spectra) leads to a distance $D = 4.8 \pm 1$ kpc. The visual lightcurve of Nova Mus 83 is extraordinary for a fast nova: After a decline over about 4 months the brightness remained constant for at least 5 months (based on data collected by the RASNZ). Until then no formation of an optically thick dust shell was observed. The prenova could be identified on the SRC *J* sky survey with a faint object of $V \geqq 21$ mag. With $\Delta m \geqq 14$ mag Nova Mus exhibits one of the largest outburst ranges ever observed for novae.

Visual spectroscopy during 10 days starting on January 21, 3 days after discovery, showed that Nova Mus had already entered the diffuse enhanced phase. The Balmer- and some metallic emission lines showed a complex structure with several emission components of a few hundred km s^{-1}, broad wings extending to ± 3000 km s^{-1}, and two P Cygni type absorption systems at -588 km s^{-1} (principal absorption) and at -1753 km s^{-1} (diffuse enhanced absorption). The 4640 Å feature is already rather conspicuous. The flux distribution (0.32–10 μm) was that of an optically thin free-free emitter. The luminosity of Nova Mus after outburst was of the order of one Eddington luminosity for a white dwarf of one solar mass.

By February 21 and 24 Nova Mus had entered the Orion phase with a radial velocity of the Orion absorption system of -1976 km s^{-1}. Typical Orion lines like He I, N II, N III, O II increased in strength between February 21 and 24, while the absorption systems considerably weakened. The [O III] λλ4959, 5007 lines, characteristic of the nebular stage are already stronger than the Fe II lines.

The UV spectra showed lines of He, N, C, O, and some metals, at a wide variety of ionization and/or excitation potentials, the strongest lines being O I λ1304 and N III] λ1750. The intercombination lines (e.g. N III], C III], Si III]) increased in strength between February 19 and March 4. No P Cygni absorption components could be found. Differences in line profiles demonstrate that the expanding envelope has a complex structure with excitation conditions being different for different regions.

The strongest lines in the IR spectral range are the hydrogen Bracket series. Several highly ionized emission lines could be identified: A broad emission feature at 1.56 μm – previously unreported – was identified as a blend of He II, O V, and N V. An O VI line was found at 1.45 μm. On the other hand, molecular lines (CO, formaldehyde) are also present. This indicates the presence of molecules associated with dust in the surroundings of Nova Mus.

Abundance ratios deduced from the IR and UV line intensities suggest an overabundance of helium (He/H ≧ 0.12) and a pronounced overabundance of nitrogen relative to carbon and oxygen (N/C ≈ 20, N/O ≈ 2.4). The abundance ratios as well as the luminosity of one L_{Edd} after outburst are entirely consistent with the thermonuclear runaway model of nova outbursts with hydrogen being burnt via the CNO cycle.

Key words: novae – spectroscopy – photometry – expanding envelopes – abundances

Send offprint requests to: J. Krautter

* Based on observations collected at the European Southern Observatory at La Silla, Chile, and on observations by the International Ultraviolet Explorer collected at the Villafranca Satellite Tracking Station of the European Space Agency

** Present address: University of South Africa, Dept of Maths and Astronomy, P.O. Box 392, 0001 Pretoria, Rep. of South Africa

Table 1. Journal of Coudé observations

Plate no.	Date	Start of exposure (JD)	Exposure time	Remarks
F 8015	January 25, 1983	24405359.83	1^h20^m	Slightly underexposed
F 8021	January 26, 1983	24405360.80	1^h01^m	Good
F 8031	January 27, 1983	24405361.82	1^h25^m	Good
F 8036	January 28, 1983	24405362.76	1^h06^m	Good
F 8038	January 29, 1983	24405363.81	1^h43^m	Slightly underexposed
F 8047	February 21, 1983	24405386.84	0^h39^m	Good
F 8060	February 24, 1983	24405389.88	1^h00^m	Good

I. Introduction

Nova Mus 1983 was discovered on 1983 January 18, by Liller (1983) as a 7th magnitude object. A general problem concerning observations of nova outbursts is that these events are unpredictable. Hence, coordinated observations over wide spectral ranges are very rare due to the difficulty to get ad hoc access to the necessary telescopes and instrumentation.

For the outburst of Nova Mus 83 the facilities of the European Southern Observatory on Cerro La Silla, Chile, with its many telescopes and widespread instrumentation, offered excellent possibilities to organize an extensive observation campaign. Here we report on spectroscopic and photometric observations, both in the visual and infrared spectral ranges obtained during 3 weeks covering the early decline phase of Nova Muscae 1983, and on UV spectral observations made with IUE several weeks after outburst.

II. Spectroscopic observations

A) Visual spectral range

Observations

Spectroscopic observations in the visual spectral range with medium and high resolution were obtained between January 21, and February 24, 1983. Coudé spectrograms of Nova Mus 1983 were secured with the Coudé spectrograph of the ESO 1.52 m telescope during the periods January 25–29 (5 spectrograms), and February 21–24 (2 spectrograms). A journal of our observations is provided in Table 1. The spectra taken in January were recorded on IIIa-J plates, the ones taken in February were recorded on IIa-O plates. The plates were baked in forming gas. The dispersion was 20 Å mm^{-1} (resolution $\sim$0.4 Å). The IIIa-J spectrograms are widened to 150 μm, the spectra recorded on IIa-O plates were widened to 200 μm (plate No. F8047), and to 250 μm (plate No. F8060), respectively. The effective wavelength ranges are 3400–5200 Å for the IIIa-J plates and 3600–5000 Å for the IIa-O plates. The plates were developed for 5 minutes in D-19 and calibrated by means of the ESO ETA spectrograph. Finally, we measured each spectrogram with the Grant measuring machine of the MPI-A at Heidelberg.

On January 21 and 23, medium resolution spectrograms in the blue spectral range with a dispersion of 59 Å mm^{-1} were obtained with the ESO 1.52 m telescope using a 3-stage EMI image intensifier attached to the Boller and Chivens Cassegrain spectrograph. The spectrograms were recorded on IIIa-J plates with a spectral resolution of about 3 Å and were calibrated using an average IIIa-J calibration curve. Unfortunately, the spectrum of January 21 is strongly overexposed and the strong emission lines are heavily saturated. For conversion into intensities the calibration curve had to be extrapolated to very high densities ($\sim$4.5). Hence, intensities of strong emission lines obtained from this spectrum are unreliable. On the other hand, line profiles of the weaker lines give useful results.

On January 22, a 39 Å mm^{-1} spectrogram was taken with the image dissector scanner attached to the Boller and Chivens Cassegrain spectrograph of the ESO 3.6 m telescope. The spectrum covers the spectral range 4000–4800 Å and has a spectral resolution of 2.5 Å. Because of the large photon flux which could have damaged the detector, we reduced the amount of energy going through the spectrograph aperture by defocussing the telescope.

High resolution spectrograms

Since our most homogeneous and comprehensive set of data are the Coudé spectrograms taken between January 25 to 29, we will start with a description of these spectra. Afterwards we will discuss the spectral variations from the medium resolution spectrograms taken earlier and the Coudé spectrograms taken in February.

We could not find any significant spectral variation between January 25 and 29. Hence, we superposed the five digitized Coudé spectrograms taken in January in order to obtain a mean spectrum with a high signal-to-noise ratio. The resulting mean spectrum of Nova Mus 1983 is shown in Fig. 1, along with the individual Coudé spectra taken in February. It should be noted that the wavelength regions longward of 4750 Å are relatively far away from the plate center and suffer from astigmatism. Furthermore, Hβ was strongly overexposed on all plates. As for the medium resolution spectrograms, conversion from density to intensity for Hβ was possible only by extrapolating the obtained calibration curves to high densities.

The spectrum is dominated by very strong emission lines, the strongest of which are the Balmer lines with P Cygni profiles. Balmer emission can be traced up to H19 and two absorption systems are clearly discernible until at least H 12. A more detailed discussion of the Balmer line profiles will be presented in connection with a discussion of the radial velocities. Apart from the hydrogen lines, P Cygni absorption has also been found in some metallic emission lines. Interstellar absorption lines of Ca II H and K are present. In addition, there is a narrow absorption which is

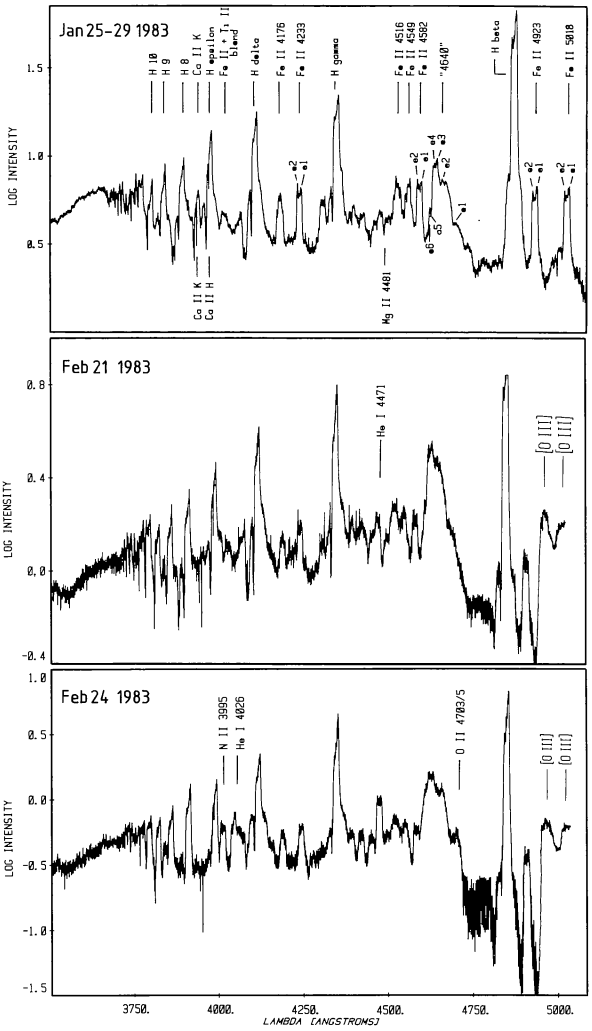

Fig. 1. High resolution spectra of Nova Muscae 1983. The upper spectrum is the mean spectrum of the Coudé spectra taken during January 25–29. The most prominent emission lines are indicated. In the two lower spectra only additional emission lines are indicated. Note that Hβ is strongly overexposed. For the upper spectrum the conversion from density to intensity was obtained by extrapolating the calibration curve. No extrapolation was done for the two spectra taken in February

practically unshifted, if identified with Mg II λ4481. This line is a transition from a non-metastable level and is very sensitive to the dilution of radiation in extended atmospheres (cf. e.g. Struve and Wurm, 1938). It is therefore very unlikely that this line can be formed in the extended envelope of a nova. We are not aware of any reasonable explanation of where this particular line could have its origin. All other lines are found in emission. Most lines are identified as lines or blends from singly ionized metals (mainly Fe II). This spectral appearance is typical for the diffuse enhanced phase of the spectral evolution of a nova. Around 4640 Å is a very strong emission feature which may be a blend of O II, N II, probably N III, and contributions from Fe II and Ti II. O II, N II, and N III lines are typical for the Orion phase of a nova. However, no further emission lines typical for this phase could be found on any of our 5 spectrograms.

Of each plate radial velocities were individually measured with the Grant measuring machine. The results for the Balmer lines and a few selected metallic emission lines are presented in Table 2. The heliocentric radial velocities of the individual plates (including the two plates taken in February) are listed in columns 3–9. The mean internal error of a single measurement on one plate was typically $2\,\mathrm{km\,s^{-1}}$ near to the plate center and $4\,\mathrm{km\,s^{-1}}$ towards the edges. However, this accuracy could only be obtained for strong, sharp absorption lines. Most emission features were difficult to localize with the Grant machine and so the resulting uncertainty may be much higher.

No systematic velocity variation could be found for any feature between January 25 and January 29. The varying radial velocities of certain features are partly due to uncertainties of the measurements, but may also be an indication of irregular small-scale variations in the nova envelope.

Two emission line systems are clearly visible in the Balmer and (unblended) metallic emission lines. The mean radial velocities of the Balmer line systems are $+531\pm58$ and $-434\pm33\,\mathrm{km\,s^{-1}}$, while those of the metallic emission lines are $+419\pm42$ and $-348\pm34\,\mathrm{km\,s^{-1}}$ indicating a possible systematic difference in radial velocities. There are also differences in the line profiles, since in the metallic emission lines the red- and the blueshifted components are of about the same strength, whereas in the Balmer lines the redshifted component is clearly stronger than the blueshifted component. This can be well seen in Fig. 2 which shows enlarged tracings of the Balmer lines from Hβ to H8 (abscissa given in $\mathrm{km\,s^{-1}}$) and of the higher Balmer lines (abscissa given in Å). On the red wings of the Balmer lines Hβ to Hε additional emission components with higher radial velocity are probably present. These systems are denoted by *e*1 and *e*2 in Fig. 2.

Two absorption systems of constant velocity over 5 days are clearly discernible in the Balmer lines (cf. Fig. 2) and in some metallic lines (e.g., Fe II λ5016), a sharp absorption component and a diffuse absorption component with higher radial velocity. The sharp absorption component which can be readily seen from Hβ to H8 is identified with the principal absorption (pa), while the broad, high velocity component is interpreted as the so-called diffuse enhanced absorption (dea) (e.g. Payne-Gaposchkin, 1957). The results of our radial velocity measurements of the principal absorption are plotted in Fig. 3. Each point represents the mean derived from five plates of the pa velocity from Hβ up to H16. The error bars denote the mean error of the mean value (H13 was measured only once and so no bar is given). The velocity progression, as implied by Fig. 3, is due to a filling effect by the emission component. The Balmer emission decreases for higher Balmer lines and consequently there is less interference with the absorption components. Note that it is evident from Fig. 3 that the *pa* for $n \geqq 10$ is relatively unaffected by emission and should represent the true velocity of the principal absorption, v_{pa}. Therefore, we calculated v_{pa} as a mean of v_{H10} to v_{H16} and found $v_{\mathrm{pa}} = -588\pm9\,\mathrm{km\,s^{-1}}$.

The velocity of the diffuse enhanced absorption showed no dependence on the Balmer quantum number. Reliable values of v_{dea} could be measured for Hβ, Hγ, Hε, and H8 (Hδ was excluded, see below) and the mean is $v_{\mathrm{dea}} = -1753\pm55\,\mathrm{km\,s^{-1}}$. On the tracings of the Balmer lines in the superposed spectrum (Fig. 2) it can be seen that the diffuse enhanced component is split into two subcomponents. Because of the low signal-to-noise ratio it was not possible to measure these features on the individual plates. On the superposed spectrum radial velocities have been measured with respect to well defined features of known radial velocities. Table 3 lists the radial velocities of these two components which are split by

Table 2. Line identification and radial velocities

Identification	λ_o [Å]	v/8015	v/8021	v/8031	v/8036	v/8038	v/8047	v/8060	Remarks
					[km s^{-1}]				
FeII 42	5018.84	+ 494	+ 524	+ 517	+ 611	+ 624			*e*1
FeII 42	5018.84	− 201	− 219	− 196	− 241	− 218			*e*2
FeII 42	4923.92	+ 405	+ 405	+ 415	+ 422	+ 432	+ 452	+386	*e*1
FeII 42	4923.92	− 285	− 332	− 311	− 309	− 324	− 237	−417	*e*2
Hβ	4861.33	+1657		+1720	+1870	+1684			*e*1
Hβ	4861.33	+ 98	+ 99	+ 96	+ 94	+ 102	+ 611	+394	*e*3
							− 492	−511	
Hβ	4861.33	− 675	− 753	− 738	− 725	− 668	− 730	−936	pa
							− 901		
Hβ	4861.33	−1457	−1581	−1613	−1631	−1538	−2094		dea/Orion
4640 blend			4681.83 Å	4681.17 Å	4682.49 Å	4680.94 Å			*e*1, HeII?
4640 blend		4665.35 Å	4660.39 Å	4663.11 Å	4661.77 Å				*e*2
4640 blend				4635.24 Å	4635.58 Å	4635.67 Å	4632.80 Å		*e*3, OII, NIII
4640 blend					4628.21 Å	4627.87 Å			*e*4, NII
4640 blend			4617.37 Å	4618.07 Å	4618.66 Å	4618.39 Å			*a*5
4640 blend					4615.70 Å	4615.13 Å			*e*6, NII
FeII 37	4582.84						+ 485	+506	*e*1
							− 335	−356	*e*2
FeII 38	4549.47	+ 491		+ 444	+ 479	+ 491			*e*1
FeII 38	4549.47	− 384	− 391	− 406	− 394	− 343			*e*2
MgII 4	4481.23	− 14	− 12	− 32	+ 8	+ 19			*a*, interst.?
HeI 4471	4471.51							+509	
								−453	
Hγ	4340.47	+1804	+1826			+1849			*e*1
Hγ	4340.47	+1127	+1272	+1272	+1314	+1135			*e*2
Hγ	4340.47		+ 596	+ 607	+ 599	+ 581	+ 561	+558	*e*3
Hγ	4340.47	− 428	− 451	− 459	− 449	− 448	− 463	−473	*e*4
Hγ	4340.47	− 676	− 676	− 656	− 693	− 690	− 736	−726	pa
							− 890	−917	
Hγ	4340.47	−1777	−1777	−1777	−1752	−1758	−1984		dea/Orion
FeII 27	4233.17	+ 369	+ 382	+ 363	+ 376	+ 402	+ 361	+475	*e*1
FeII 27	4233.17	− 357	− 340	− 342	− 351	− 352	− 384	−435	*e*2
Hδ	4101.74		+2376	+2440	+2174	+2283			*e*1
Hδ	4101.74	+ 411	+ 494	+ 561	+ 563	+ 560	+ 545	+543	*e*3
Hδ	4101.74	− 434	− 398	− 419	− 422	− 451	− 471	−469	*e*4
Hδ	4101.74	− 649	− 632	− 635	− 643	− 656	− 716	−718	pa
							− 889	−895	
Hδ	4101.74	−2106	−2007	−2056	−1956	−1962	−2089		dea/Orion
Hε	3970.07	+1952	+2146	+1930	+1896	+1783			*e*1
Hε	3970.07	+ 446	+ 397	+ 530	+ 540	+ 529	+ 519	+531	*e*2
CaII H	3968.47	− 20	− 12	− 17	− 11	− 17	− 11	− 18	*a*, interst.
Hε	3970.07	− 684	− 699	− 691	− 696	− 685	− 744	−725	pa
							− 892	−953	

1984A&A...137..307K

Table 2 (continued)

Hε	3970.07	−1729	−1769	−1790	−1739	−1688	−1923		dea/Orion
CaII K	3933.66	+ 365	+ 390	+ 363	+ 315	+ 403			*e*
CaII K	3933.66	− 18	− 15	− 13	− 12	− 17	− 17	− 8	*a*, interst.
CaII K	3933.66		− 675	− 677	− 673	− 682	− 570	−560	*a*
H8	3889.05	+ 542	+ 538	+ 536	+ 526	+ 541	+ 494	+526	*e*1
H8	3889.05	− 339	− 432	− 434	− 467	− 477	− 421	−452	*e*2
H8	3889.05	− 612	− 617	− 656	− 671	− 673	− 711	−751	pa
							− 895	−907	
H8	3889.05	−1866	−1916	−1844	−1875	−1828	−1949		dea/Orion
H9	3835.39	+1181		+ 922	+ 857	+ 977			*e*(H9)1
H9	3835.39	+ 477	+ 488	+ 487	+ 508	+ 512	+ 472	+512	*e*(H9)2
H9	3835.39		− 687	− 681	− 682	− 676	− 789	−457	pa(H9)
								−702	
H9	3835.39	−1859	−1855	−1888			−1930		dea(H9)
H10	3797.90			+ 759	+ 730				*e*(H10)1
H10	3797.90	+ 475	+ 417	+ 498	+ 482	+ 488	+ 465	+535	*e*(H10)2
H10	3797.90		− 371	− 341		− 367	− 445	−468	*e*(H10)3
H10	3797.90	− 574	− 571	− 595	− 661	− 669	− 580	−572	pa(H10)
							− 708	−716	
H11	3770.63	+ 484	+ 403	+ 434	+ 499	+ 506	+ 599		*e*(H11)1
H11	3770.63	− 298	− 312	− 298				−442	*e*(H11)2
H11	3770.63		− 561	− 589	− 595	− 652	− 558	−580	pa(H11)
							− 715	−699	
H12	3750.15	+ 538	+ 533	+ 548	+ 520	+ 561			*e*(H12)
H12	3750.15	− 557	− 556	− 570	− 583	− 572	− 586	−561	pa(H12)
							− 716		
H13	3734.37	− 424	− 439	− 428	− 439	− 424			*e*(H13)
H13	3734.37		− 569				− 585		pa(H13)
							− 703		
H14	3721.94	− 259	− 269	− 286		− 254			*e*(H14)
H14	3721.94		− 566	− 595	− 589	− 597	− 595		pa(H14)
							− 710		
H15	3711.97	− 155		− 159	− 151	− 149			*e*(H15)
H15	3711.97	− 545	− 549	− 567	− 565	− 553	− 600		pa(H15)
							− 581		
H16	3703.86		− 580	− 636		− 644	− 718		pa(H16)

Notes:
1) The numbers behind *v* in the first line denote plate numbers.
2) The fastest absorption component refers to the diffuse enhanced (dea) phase for the spectra of January and to the Orion phase for the spectra taken in February, respectively.
3) For the 4640 Å blend only the measured wavelengths with tentative line identifications are given

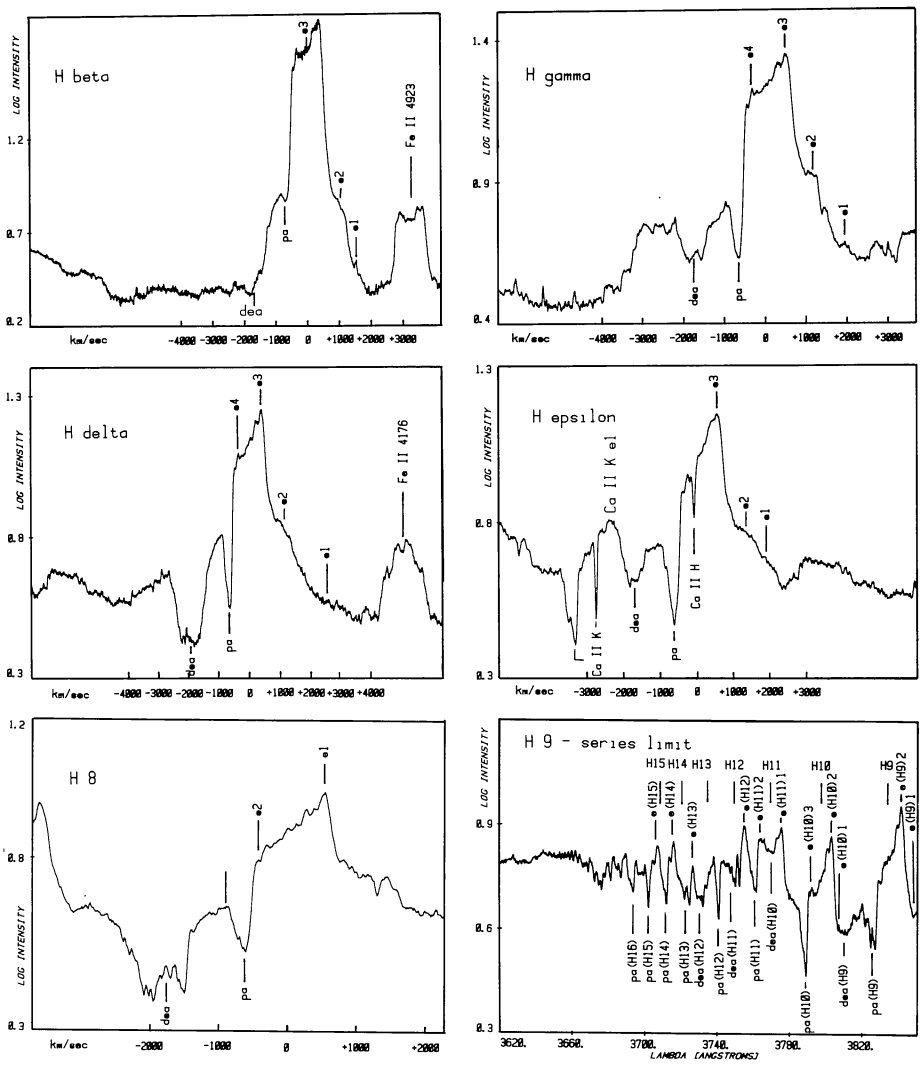

Fig. 2. Balmer-line profiles of Nova Muscae 1983. Each profile is a superposition of five spectrograms

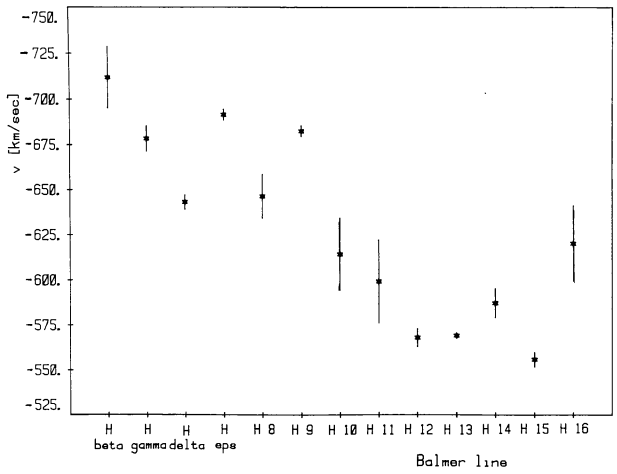

Fig. 3. Radial velocities of the principal absorption components

an average velocity of 328 km s^{-1}. The appearance of several subcomponents in the dea spectrum is a rather common phenomenon in novae during the diffuse enhanced phase (e.g. Mc Laughlin, 1960).

Table 3. Radial velocities of diffuse enhanced absorption components

	a_1	a_2
	[km s^{-1}]	
Hβ	−1501	−1796
Hγ	−1544	−1833
Hδ	−1832	−2196
Hε	−1554	−1794
H8	−1545	−1995

For Hδ the dea component is systematically stronger and more blueshifted than the other Balmer dea components. This could be attributed to a possible contribution of an absorption component of the N III λ4097 line which is typically found in the Orion phase. However, no indications for an emission component of this line nor of N III λ4103 is detectable. All these spectral properties show that Nova Mus 1983 was during January 25–29 in a transition stage between the diffuse enhanced and the Orion phase.

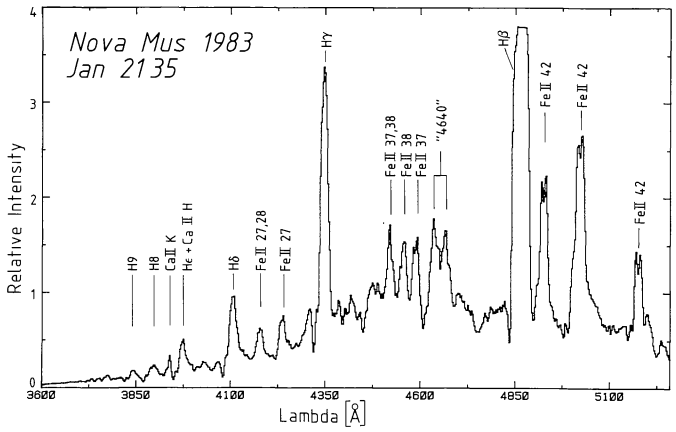

Fig. 4. Image tube spectrum taken on January 21.35. The stronger emission lines are heavily saturated

All emission lines show extended line wings, in some cases up to about $\pm 3000\,\mathrm{km\,s^{-1}}$, as is evident from the velocity scale in Fig. 2. This is less obvious for the metallic emission lines. More accurate values could not be determined because of the large number of emission lines which causes severe blending in the line wings.

On all five spectrograms we measured the radial velocities of the interstellar Ca II H, and K absorption lines and derived a mean value of $v_H = v_K = 15 \pm 2\,\mathrm{km\,s^{-1}}$.

Medium resolution spectrograms

As an example of the medium resolution spectrograms our first spectrogram taken on January 21 in the 3600–5000 Å wavelength range is presented in Fig. 4. These spectra are rather similar to those taken 4–8 nights later. The radial velocities of the emission and of the diffuse enhanced absorption components are, within the error limits, the same as for the Coudé spectra, with the exception of Hδ where the dea component is not found at shorter wavelengths than the other dea lines. The mean radial velocity of the principal absorption component is systematically higher which is probably caused by the lower resolution. The strength of the diffuse enhanced absorption component varies; it is largest on January 21 and is clearly weaker on the spectrum taken on January 23 reaching about the strength found in the Coudé spectra. However, due to the different resolution, a comparison can be only very rough. On the basis of our medium resolution spectra Nova Mus 83 seems to be in the diffuse enhanced stage during January 21–23. However, we would like to note that already on January 21 the 4640 Å feature is rather strong.

Orion phase

By February 21, some remarkable changes took place in the spectral appearance of Nova Mus 1983 (cf. Fig. 1) showing that it has now entered the Orion stage. The metallic emission lines became slightly weaker. HeI λλ4026, 4471 emission lines are visible and have about the strength of the metallic emission lines. Also a weak emission of HeII λ4686 is now present as well as NII λ3995, which is a characteristic feature of the Orion phase. Apart from the Balmer lines the most conspicuous feature is the 4640 complex. Already present in considerable strength are the forbidden [OIII] λλ4959, 5007 emission lines which are characteristic of the last stage of the nova evolution, the nebular stage. This early appearance of the [OIII] lines is somewhat unusual, since according to McLaughlin (1960) these lines should reach the same strength as the Fe II lines 4.4 mag below maximum brightness.

Changes also took place in the absorption systems. The fast absorption system has increased its radial velocity compared to the value at the end of January (-1976 ± 70 instead of $-1753 \pm 55\,\mathrm{km\,s^{-1}}$). This system is the Orion absorption system which usually has a larger radial velocity than the diffuse enhanced system. Again the absorption component of Hδ is stronger and at higher velocities than the other fast absorption components, giving strong evidence for the presence of NIII absorption. However, no other absorption lines of HeI, NII, or OII, which are characteristic of the Orion absorption system could be identified. The principal absorption system is still present in the Balmer lines but is now split into two components which are on the average separated by $147 \pm 23\,\mathrm{km\,s^{-1}}$. Faint indications of this splitting can in fact be already traced in the line profiles of Hε, H8, and especially H9 in the January spectra (cf. Fig. 2). This behaviour can be easily explained by variations in the relative line strengths as has also been found for other novae (McLaughlin, 1960).

Three nights later, on February 24, further changes have taken place. Most remarkable is the weakening of the absorption systems, both of the fast absorption and of the principal absorption, and the increase of the HeI λλ4026, 4471 line strength. Especially HeI λ4471 is now considerably stronger than the metallic emission lines. Other lines characterising the Orion stage have increased in strength, too, like NII λ3995 and OII λλ4703, 4705. While the Balmer lines are still very broad (with extended wings), the HeI λ4471 emission line has a comparatively small total line width of only $1550\,\mathrm{km\,s^{-1}}$.

B) UV spectroscopy

UV spectrograms were obtained on February 19, and March 4, 1983, with the IUE satellite using the facilities of the ESA Villafranca ground station. On February 19, a spectrogram in the low resolution mode was taken with the SWP camera. On March 4, several spectra both in the short and long wavelength range were obtained in both low and high resolution mode. All spectra were taken through the large aperture. The journal of our IUE observations is given in Table 4. In the present paper only a preliminary discussion of the UV data will be given. A more detailed discussion will be presented in a forthcoming paper (Wargau, 1984).

Low resolution spectra

Figure 5 shows a tracing of the low resolution spectrogram of Nova Mus 83 together with some line identifications. The tracing is a combination of the SWP ($\lambda \leqq 1950$ Å) and LWR ($\lambda > 1950$ Å) spectrograms taken with 5 min exposure times on March 4 (SWP 19384 and LWR 15421). Note that the spectrum has not been corrected for interstellar reddening.

The continuum energy distribution has been used to determine the interstellar extinction from the 2200 Å feature. However, because of the low exposure level of the continuum and because of the presence of many weak emission lines, the derived extinction is somewhat uncertain. A smooth continuum was obtained for $E_{B-V} = 0.45 \pm 0.15$ in reasonable agreement with $E_{B-V} = 0.40$ determined from an interstellar extinction map in the visual spectral range (see below). In the following we shall use the value of 0.45 mag for dereddening of our data.

Table 4. Journal of IUE observations

Image no.	Date (UT)	Camera	Resolution	Expos. time [min]	Remarks
19299	1983, February 19.561	SWP	Low	20	Em. lines saturated
19383	1983, March 4.176	SWP	Low	20	Em. lines saturated
15421	4.192	LWR	Low	5	
19384	4.211	SWP	Low	5	
19385	4.232	SWP	Low	2	
19386	4.250	SWP	High	120	Continuum underexposed
15422	4.356	LWR	Low	0.5	
19387	4.358	SWP	High	20	Underexposed
19388	4.397	SWP	Low	0.5	Continuum underexposed
15423	4.406	LWR	High	45	
19389	4.441	SWP	High	12	Underexposed

The spectrum shows that the nova is at the end of the transition stage, and is about to enter the nebular phase. The spectrum is dominated by strong emission lines the strongest of which are saturated due to the low dynamic range of the IUE detector. Many weak emission lines are present besides the strong lines. The strongest emission lines are O I λ1304, and N III] λ1750. Dominant are emission lines from neutral, singly or doubly ionized atoms. Lines from highly ionized atoms and/or excited levels are present too, but weaker than the other lines. Very conspicuous are intercombination lines like N III] λ1750, N IV] λ1486, C III] λ1908, Si III] λ1892, and O III] λ1663.

A quantitative comparison of the SWP spectrum taken on February 19, 1983 (SWP 19299) with one of the SWP spectra taken two weeks later on March 4, 1983, is not possible, since the former is highly saturated (exposure time 20 min). However, a comparison with the similarly overexposed 20 min exposure SWP spectrum taken in March (SWP 19383) gives clear evidence that the strength of the intercombination lines increased considerably, indicating a decrease of the electron density in the envelope.

Following the procedure applied by Williams et al. (1981) for the recurrent nova U Sco it is possible to derive from the strength of the CNO lines crude abundance ratios relative to each other. The emission lines of C, N, and O are all collisionally excited.

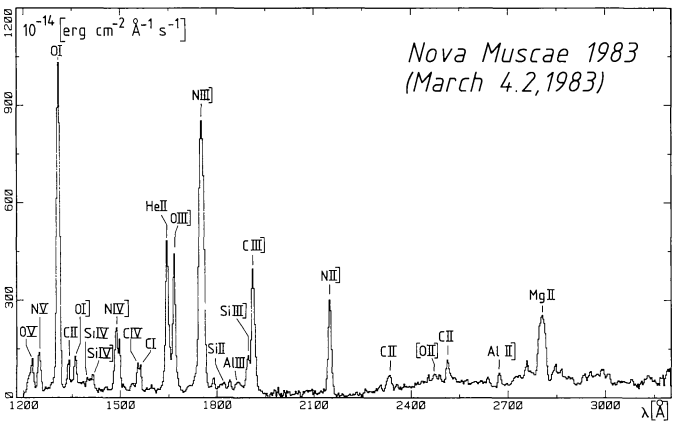

Fig. 5. The combined SWP and LWR UV spectrograms taken with 5 min exposure time. The more significant emission features are indicated

Hence, under the simplifying assumption, that ionizations of C, N, and O, are similar, i.e. that $C^{+3}/N^{+3} \approx C/N$ and $N^{+2}/O^{+2} \approx N/O$, approximate abundance ratios can be calculated from the relative line strengths of C IV/λ1549/N IV] λ1486 and N III] λ1750/O III] λ1663. For these four ions critical densities for de-excitation are $>10^9$ cm^{-3} (cf. Baldwin and Netzer, 1978). On the other hand, in the Coudé spectra taken about 10 days earlier the [O III] lines are already present. Since these lines are collisionally de-excited above electron densities $N_e \approx 6.5\,10^5$ cm^{-3} (Osterbrock, 1974), the gas density in the shell must be lower than this value. Hence, collisional de-excitation processes can be neglected. After deconvolution of the blended lines, the observed line ratios are $F(\lambda1750)/F(\lambda1663) \approx 5.9$ and $F(\lambda1549)/F(\lambda1486) \approx 0.3$. Using Williams et al.'s relations [Eqs. (2) and (3) of their paper]

$$n(N^{+2})/n(O^{+2}) = 0.5 \exp[-4305/T_e] \cdot F(\lambda1750)/F(\lambda1663)$$

and

$$n(C^{+3})/n(N^{+3}) = 0.2 \exp[-3942/T_e] \cdot F(\lambda1549)/F(\lambda1486)$$

and assuming $T_e \approx 2\,10^4$ K one obtains the abundance ratios $N/C \approx 20$ and $N/O \approx 2.4$. The results are not very sensitive to the adopted T_e, since $T_e = 10^4$ K leads to abundance ratios of $N/C = 25$ and $N/O = 2.0$, differing by only 20%. By comparing these values with solar abundance ratios N is overabundant relative to C by a factor of 80, and compared to O by a factor of 15.

The nitrogen abundance ratio relative to C and O is rather high as compared with other novae. For instance, for DQ Her $N/C = 4.3$ and $N/O = 0.9$ has been found (Williams et al., 1978), and for Nova Cyg 1978 values of 2.6 and 1.2, respectively, were derived (Stickland et al., 1981). Recently the same abundance ratio $N/C = 20$ has been determined for Nova CrA 1981 by Williams (1983). Williams (1982) reports similar abundance ratios for CP Pup, namely $N/O \geqq 10$ and $N/C \geqq 10$. However, since only lower limits could be derived by Williams, the abundance ratios in CP Pup might be even more extreme.

Unfortunately no abundance ratios of CNO relative to H could be determined, since the intensity of the hydrogen lines at the time of our UV observations is not known. Hence, a comparison

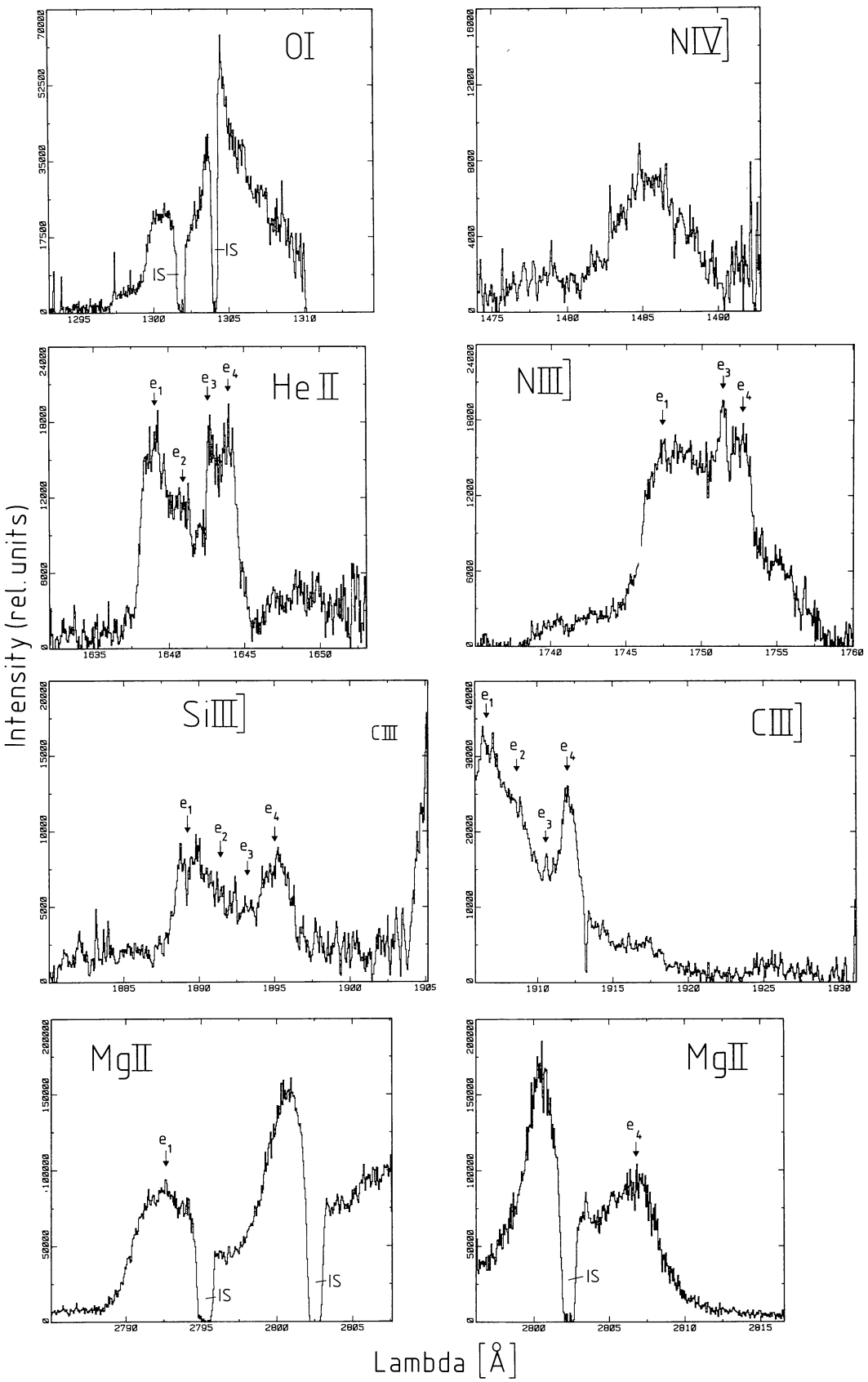

Fig. 6. Line profiles of the most prominent emission lines from the high resolution UV spectrograms

Table 5. UV-radial velocities of UV lines (from high resolution spectrum SWP 19386 with 120^m exposure time. N III] is from SWP 19837 with 20^m exposure time)

	λ_0	e_1	e_2	e_3	e_4
		[km s^{-1}]			
He II	1640	−310	−20	+275	+600
N III]	1750	−377		+288	+520
Si III]	1892	−380	−30	+190	+510
C III]	1909	−319		+293	+511
Mg II	2795	−268			+492
	2802				

with solar abundances is not possible. On the other hand, since the CNO lines are very strong, it does not seem unreasonable to suspect that CNO may be overabundant with respect to the sun.

High resolution spectrograms

Our high resolution spectrograms are underexposed and hence only few emission lines are usable for a detailed discussion. Unfortunately, some of the lines do not allow a detailed study of their profile because of blending with other lines or because of the doublet or multiplet character of the line itself. Figure 6 shows tracings of the best exposed emission lines. N III] λ1750 has been taken from the spectrum with 20 min exposure time.

Best suited for line profile studies are He II λ1640, N III] λ1750, Si III] λ1892, and C III] λ1908. The Mg II λλ2795, 2802 doublet gives some information, because of the comparatively wide separation of the two components. These emission lines show 4 emission components, whose radial velocities are listed in Table 5 and marked by arrows in Fig. 6. The strongest emission components have radial velocities of +540 km s^{-1} and −320 km s^{-1}. This is in good agreement with the velocities determined in the visual spectra. Two faint components of lower radial velocities are present too, but they are only barely detectable in some lines. These two components (*e*2 and *e*3) have not been found in the visual spectral range, the reason probably being the lower spectral resolution of our Coudé spectra.

The mean total line width of 1470 km s^{-1} of the 3 lines He II, Si III], and C III] is smaller than the line widths found for the emission lines in the visual spectra. No broad line wings can be seen in the UV spectral region. A simple explanation may be that the *S*/*N* of the high resolution UV spectrograms is too low. On the other hand, in the February Coudé spectra He I λ4471 and [O III] λ4959 do not seem to have the same broad wings as the other lines. This may indicate that in fact the broad line wings disappeared or became considerably weaker.

The N IV] λ1486 line displays a line profile which differs considerably from that of the other emission lines, including the other intercombination lines. It does not show the 4 component emission structure with minimal intensity in the line center, but rather a symmetric profile with maximal intensity in the center. This cannot be an effect of the lower signal to noise ratio of this line, since in our shorter exposed high resolution spectrum e.g. He II λ1640 has about the same signal to noise and clearly shows the four component structure. This finding could be an indication that the lines of the more highly ionized atoms have different line profiles than those of neutral, singly, or doubly ionized atoms. These different line profiles probably reflect different geometries of their respective emission region.

It is interesting to note that no P Cygni absorption, neither principal nor diffuse enhanced, could be detected. A simple explanation may be that the continuum level is too weak and the signal-to-noise ratio too low in order to detect any absorption component. Alternatively, one may not exclude that the absorption systems had already disappeared or had considerably weakened by the time the UV spectrogram was taken. This is supported by the weakening of the diffuse enhanced absorption components in the visual spectral range from February 21 to 24.

Several interstellar lines could be found in our spectrograms. These lines are indicated in Fig. 6. The lines are saturated and no useful limit of E_{B-V} could be determined.

C) The IR spectrum

Observations and data reduction

Low resolution ($R \sim 70$) infrared spectra of the nova between 1.43 μm and 4.15 μm have been obtained in the period January 31–February 10, 1983 with the ESO CVF spectrophotometer mounted on both the 3.6 m and 1 m ESO telescopes. The data have been calibrated by measuring at least one standard star at similar airmass and in the same spectral points. The absolute fluxes of the standard stars were determined by taking the nearest broad band photometric point and scaling according to a black-body law of temperature equal to $T_{\rm eff}$.

Due to the low spectral resolution (equivalent to about 4000 km s^{-1}) all the observed lines are unresolved. The line intensities have been determined by fitting to the observed points a gaussian instrumental profile over a straight continuum. For the brighter lines, all the line parameters (amplitude, central wavelength and width) are defined by means of a minimum chi-square method. In the case of faint lines, both the line width and central wavelength have been fixed. The error on the line amplitude is computed according to the standard method based on the chi-square variation (e.g. Avni, 1976). This is the error quoted in all the tables. A further uncertainty of about 10% on the absolute line intensities comes from the flux calibration. However, it does not affect at all the relative quantities, such as line ratios and equivalent widths.

The wavelength calibration of the CVF has been obtained in the laboratory using a monochromator. A further calibration check has been carried out by comparing the fitted wavelengths of observed hydrogen lines with respect to the theoretical values. In such a way, all the systematic errors are eliminated and a residual scatter of about 0.4% was found in the various measurements. Therefore, a line has been identified when the observed and predicted wavelengths differed by less than 0.4%.

Hydrogen lines

The nova was monitored during a period of 10 days (January 31–February 10) in the hydrogen recombination lines Bα (5–4, 4.0512 μm) and Bγ (7–4, 2.1655 μm). Two measurements were also obtained for the Bζ (10–4, 1.7362 μm) line. Table 6 lists the observed intensities and equivalent widths. We expect a negligible contamination from He II 10–9 (4.0512 μm) to Bα and from C IV 9–8 (1.737 μm) to Bζ, the expected intensities being about $3\,10^{-13}$ erg cm^{-2} s^{-1} and $<3.4\,10^{-12}$ erg cm^{-2} s^{-1}, respectively (cf. Table 7).

Table 6. Hydrogen and HeI lines

Date	Telescope	Line	Obs. intensity (10^{-11} erg cm^{-2} s^{-1})	Obs. eq. width[a] (μm)
31 January	3.6 m	Bα	16.1 (±0.4)	0.338
31 January	3.6 m	Bγ	8.65(±0.26)	0.0733
02 February	3.6 m	Bα	20.7 (±0.5)	0.442
02 February	3.6 m	Bγ	11.1 (±0.1)	0.0810
02 February	3.6 m	Bζ	4.21(±0.14)	0.0231
07 February	1 m	Bα	11.3 (±0.6)	0.45 (±0.15)
07 February	1 m	Bγ	7.12(±0.35)	0.0907
10 February	1 m	Bα	15. (±3.)	Undefinable
10 February	1 m	Bγ	7.7 (±1.)	0.10 (±0.02)
10 February	1 m	Bζ	3.6 (±0.1)	0.029
10 February	1 m	HeI 2^1S-2^1P	7.4 (±0.7)	0.09 (±0.02)

[a] Where not quoted, the errors are less than 5%

The ratio Bγ/Bα is always larger than that expected for thin gas emission (0.24–0.35), indicating that the lines are self-absorbed, but it is lower than expected in a completely thick case (>0.9). The growth of this ratio during the last days indicates an increase of the optical depth in the lines.

The observed equivalent widths are uniformly increasing, showing the stellar contribution becoming fainter with time, as one expects when the nova moves towards the nebular stage. The equivalent widths of Bγ and Bζ are always near to the values computed assuming thermodynamic equilibrium in the level population and pure $f-f$ continuum emission (0.09 and 0.03, respectively). The low value observed in Bα (=0.4 against 0.9) may indicate that dust emission is already important at 4 μm.

HeI lines

A very bright HeI line, namely the 2^1P-2^1S (2.058 μm) transition, has been detected in the K-band spectrum (see Fig. 8). We discuss this line separately because of its particular nature.

This transition occurs between the fine structure of the first singlet level. The population of the 2^1P level strongly depends on the optical depth of the nebula in the HeI 2^1P-1^1S (584 Å) line, which is the equivalent of the hydrogen Lyman-alpha line. If the nebula is very thick for 584 Å photons, then the ground state 1^1S "disappears" and all the recombinations to the 2^1P level end up with a 2.058 μm photon.

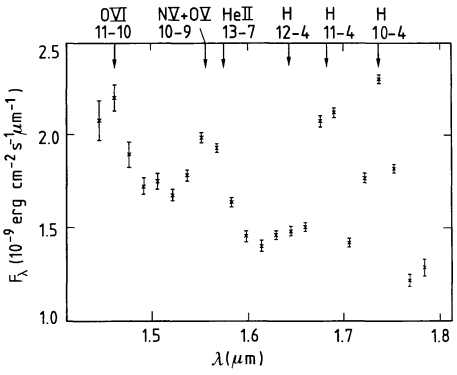

Fig. 7. 1.43–1.80 μm spectrum of Nova Muscae 1983. The intensity scale is in units of 10^{-9} erg cm^{-2} s^{-1} μm^{-1} and identified lines are indicated on top of the spectrum

The observation of such a strong line (cf. Table 6) clearly indicates that the gas must be very opaque to 584 Å photons. This is strong evidence in favour of an ionization bounded region, at least as far as the He-ionizing photons are concerned.

Quantitative results about the He^+ abundance are difficult to obtain from this line because the HeI 2^1P-1^1S photons can be absorbed by neutral hydrogen photoionization. This effect decreases the population rate of the 2^1P level, and it is strongly dependent on the detailed ionization structure of the nebula (e.g. Osterbrock, 1974). However, assuming that none of these photons is absorbed by hydrogen, an upper limit for the 2.058 μm emission coefficient, and thus a lower limit for the He^+ abundance, can be easily obtained. In such a case the population rate of the 2^1P level is about $4\,10^{-14}\,T_a^{-0.7}$ cm^3 s^{-1} (where $T_a = T_e/10{,}000$ K, Burgess and Seaton, 1960). Thus, the line emission coefficient can be written as

$$I(\text{HeI}\,2.058\,\mu\text{m}) = 3.9\,10^{-26}\,T_4^{-0.7}\int n(\text{He}^+)n_e dV \text{ erg cm}^{-2}\text{ s}^{-1}$$

which, compared to the emission coefficient for Bγ,

$$I(\text{B}\gamma) = 5.6\,10^{-27}\exp(0.32/T_4)\,T_4^{-1.5} \cdot \int n(\text{H}^+)n_e dV \text{ erg cm}^{-2}\text{ s}^{-1}$$

gives

$$n(\text{He}^+)/n(\text{H}^+) > 0.14\,T_4^{-0.8} \cdot \exp(0.32/T_4)\,I(\text{HeI}\,2.058\,\mu\text{m})/I(\text{B}\gamma).$$

In our case, assuming a reasonable electron temperature $T \approx 20{,}000$ K, we obtain a lower limit for the He^+ abundance,

$$n(\text{He}^+)/n(\text{H}^+) \geqq 0.10.$$

Complete spectrum

A complete spectrum in the H (1.4–1.80 μm), K (1.95–2.45 μm) and L (3.2–4.15 μm) atmospheric windows has been obtained during the night of February 9–10, at the 1 m ESO telescope. Figures 7–9 show the resulting data together with the positions of the known

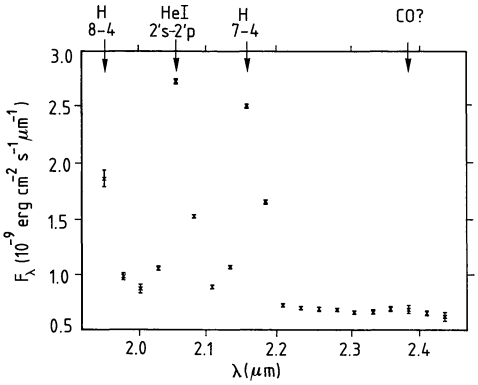

Fig. 8. 1.95–2.45 μm spectrum of Nova Muscae 1983. The intensity scale is in units of 10^{-9} erg cm^{-2} s^{-1} μm^{-1} and identified lines are indicated on top of the spectrum

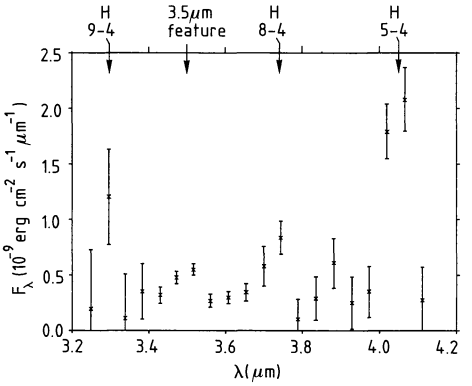

Fig. 9. 3.2–4.15 μm spectrum of Nova Muscae 1983. The intensity scale is in units of 10^{-9} erg cm^{-2} s^{-1} μm^{-1} and identified lines are indicated on top of the spectrum

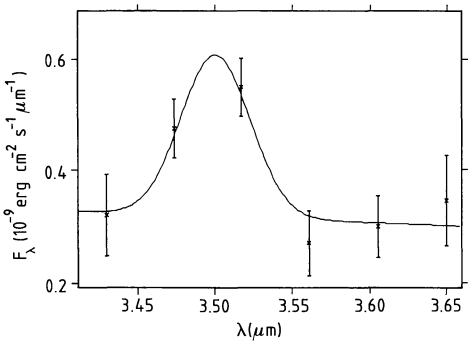

Fig. 10. The 3.5 μm feature fitted with a line having the instrumental width. The obtained intensity is listed in Table 7

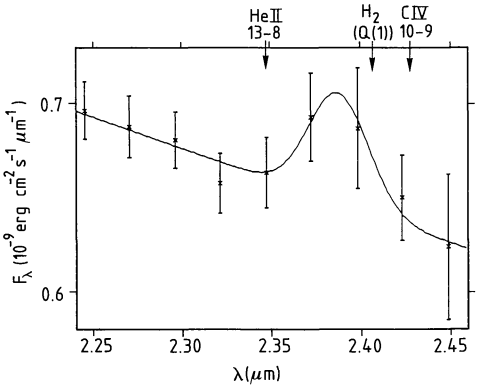

Fig. 11. The unidentified 2.39 μm feature fitted with the instrumental profile. The detection is at the 2-σ level (cf. Table 7) and the nearest known transitions are indicated on the top of the spectrum

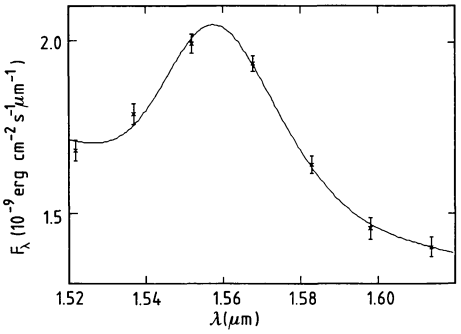

Fig. 12. The 1.56 μm broad feature fitted with the Gaussian lines having the instrumental half-width of 0.017 μm. The best fit (minimum χ^2) central wavelengths are $\lambda_0 = 1.557$ μm and $\lambda_0 = 1.575$ μm. The corresponding line intensities are listed in Table 7

transitions. The strongest lines can be identified as hydrogen and HeI transitions (see above). The bright feature at 1.56 μm is new, however, and can be interpreted in two ways:

1) A molecular emission feature

It is well known that molecules in grain mantles emit broad line systems at *IR* wavelengths (e.g. Allamandola et al., 1979). The detection of the 3.5 μm feature (Fig. 10), not coincident with any reasonable ionic line, may support this idea. In fact, it was already observed in another nova (Grasdalen and Joyce, 1976), in pre-main sequence stars (Allen et al., 1982) and it has been interpreted as emission from UV-excited formaldehyde (Blades and Whittet, 1980). Moreover, another feature, around 2.39 μm, is marginally detected at the 2-σ level in our spectrum (Fig. 11). A similar feature was found in the spectrum of Nova Vul 1976 by Ferland et al. (1979). They interpret this feature as emission from CO molecules. This may be a further proof of the presence of a strong dust component in the envelope of Nova Mus.

However, no molecular feature has ever been observed at 1.56 μm. The nearest known feature lies at 1.53 μm and was observed in a cool, C-rich Mira star (Goebel et al., 1981). Therefore, if the 1.56 μm feature does arise in grain mantles, the molecule(s) responsible has not yet been found in other astronomical situations.

2) The blend of two (or more) lines

Figure 12 shows a two line fit to the 1.56 μm feature. The most probable central wavelengths of the two lines are 1.575 μm and 1.557 μm and their intensities are listed in Table 7. They can be identified as HeII 13–7 (1.573 μm) and "XV" 10–9 (1.554 μm)

Table 7. IR line identification and line parameters

λ (μm)	Line	Obs. intensity[a]	Predicted intensity[b]		Comments
			Thin	Thick	
1.451	OVI 11–10	1.3 (0.7)	1.3	1.3	Bad atmosphere
1.477	HeII 9–6	<0.7	4.2	0.71	Bad atmosphere
1.554	(NV+OV) 10–9	1.3 (0.1)	1.3	1.3	
1.573	HeII 13–7	0.36 (0.09)	0.36	0.36	
1.693	HeII 12–7	<0.7	0.53	0.32	Close to Bη
1.737	CIV 9–8	???	<0.26	<0.34	Coincident with Bζ
1.979	(NV+OV) 14–12	<0.4	0.04	0.38	Blended with Bδ
2.101	(NV+OV) 11–10	<0.4	0.39	0.48	Blended with HeI (2.06 μm) and Bγ
2.189	HeII 10–7	<0.2	1.3	0.12	Blended with Bγ
2.347	HeII 13–8	<0.11	0.24	0.11	
2.39	CO??	0.25 (0.11)	–	–	
2.429	CIV 10–9	<0.11	<0.11	<0.11	
3.5	Formaldehyde?	1.8 (0.5)	–	–	
3.545	HeII 13–9	<1.	0.17	0.03	
3.594	(NV+OV) 13–12	<1.	0.15	0.08	
3.850	OVI 15–14	<1.	0.10	0.05	
4.051	HeII 10–8	???	0.83	0.03	Coincident with Bα

[a] In units of 10^{-11} erg cm^{-2} s^{-1}. Both the errors and the upper limits are at the 1-σ level

[b] The predicted intensities are normalized, for each ion, to the line observed with the best S/N ratio

transitions, where "XV" 10–9 is the quasi hydrogenic transition of an element in the 5th ionization state. This kind of line has already been observed in other objects, like Wolf-Rayet stars (Aitken et al., 1982) where the "XIV" (generally identified as CIV) and HeII lines show up in the spectrum. Nevertheless, no "XV" line has ever been detected so clearly in an IR spectrum.

Although the nature of the "X" element cannot be defined by the IR spectrum alone, we can reasonably restrict our choice to the most abundant C, N, O elements. The CV has a very high ionization potential (392 eV) and its abundance is thus likely to be very low, compared to the lower ionization potential ions NV (98 eV) and OV (114 eV). Also, if the CV were abundant, then one would expect a large amount of CIV to be present (unless the ionization spectrum is very peculiar) whose 10–9 line at 2.429 μm should appear bright in the IR-spectrum. Since no CIV is detected in our spectrum, we can reasonably rule out the possibility of CV contribution to the 1.554 μm line.

A possible confirmation of the presence of highly ionized species is the marginally detected line at about 1.45 μm, which can be identified as OVI 11–10 (1.451 μm) although, unfortunately, the atmospheric transmission is poor in this wavelength region.

If the interpretation of the 1.56 μm feature as HeII+NV+OV lines is correct, it may seem strange that such highly ionized species may appear in a spectrum together with molecular emission. However, a similar situation is found in the UV spectrum, where both the OI, HeII, and NV are clearly detected (cf. Sect. IIB). A simple explanation is to suppose that the very hot nova ionizes only a small region around it, where the HeII and NV lines are produced. The molecules may then be formed, as already proposed by Ferland et al. (1979), in a largely neutral cooler region extending to the outer edges of the envelope. There is, however, an alternate possibility: further away from the nova, there is material deposited by the stellar wind arising from the accretion disk/white dwarf region during the minimum phase (e.g. Krautter et al., 1981). This cooler gas component contains dust with associated molecules which can be excited by the UV radiation produced in the central region and then emit the observed 3.5 μm feature. This idea is partially supported by the evidence of an ionization bounded HeI region (see above).

Actually, from the data we have it is impossible to decide between the above two interpretations (i.e. molecular vs. ionic lines). However, the second one does not require the introduction of any new molecular species and a simple atomic theory is enough to explain the observations. We therefore prefer the ionic lines explanation.

Following it, one can compare the measured line intensities with the upper limits of other similar recombination lines expected to fall in the observed wavelength range, and obtain useful information either about the gas optical depth in the IR-transitions or about the ion abundances. In particular, an estimate of the gas optical depth can be easily made by modelling the observed intensities of HeII, NV+OV, OVI according to two extreme assumptions.

a) Gas totally opaque in the lines [i.e. $\tau(\text{line}) \to \infty$]. In the first approximation the line flux is simply proportional to the source function at the line wavelength times the surface on which $\tau(\text{line}) \approx 1$. Assuming LTE in a strongly accelerated wind, the relative line intensities of a single ion scale approximately as $(\lambda_1/\lambda_2)^{-3}\ (m_1/m_2)^{2/3}\ (A_1/A_2)^{1/3}$, where λ_1, λ_2 are the central wavelengths, m_1, m_2 are the upper level principal quantum numbers, and A_1, A_2 are the transition probabilities for the two lines, respectively (for more details cf. Felli et al., 1982; Oliva and Panagia, 1983).

b) Gas completely thin in the lines [i.e. $\tau(\text{line}) \to 0$]. All the lines considered here come from transitions between quasi-hydrogenic levels. Therefore, the theoretical intensities can be easily computed

according to well known atomic theory. In particular, the ratio of two lines is proportional to the ratio of the central wavelengths times a coefficient containing the relative level population and transition probabilities.

In brief, in the thick case one expects line intensities rapidly decreasing with wavelength. In the thin case, on the other hand, no strong correlation between central wavelength and line intensity exists.

In Table 7 the observed intensities are listed together with those obtained adopting the simple theory just described (LTE at 20,000 K is assumed). The predicted fluxes are normalized for each ion to the line observed with better accuracy.

The He II emission must arise in a thick gas to explain the missing He II 10–7 (2.189 μm), He II 13–8 (2.347 μm) and He II 9–6 (1.477 μm) lines expected adopting a thin gas emission.

No direct conclusion can be inferred for the other ions. However, the ionization potentials of N V (98 eV), O V (114 eV), O VI (138 eV) are higher than that of He II (54 eV). These ions, therefore, can be photoionized, and then produce the observed recombination lines, only in a region smaller than, and at least as opaque as the He II region.

The model suggested, therefore, is one in which the gas density decreases rapidly with distance from the star. The less numerous high-energy photons ionize only a small, dense region close to the star, where the He II, N V + O V, O VI lines are produced. The more numerous "low" energy photons can ionize a larger and less dense region, where the bulk of the H and He I lines are produced.

In such a situation, the relationship between line intensity and ion abundance is not direct, the thick emission depending on the details of the gas distribution. In particular, the line flux is not any more proportional to $n_{\rm ion} n_e V$, as in the thin condition, because the part of the gas inside the $\tau \approx 1$ region does not contribute to the line emission. Therefore, the ion abundances deduced assuming thin emission are lower than the real abundances.

Furthermore, when lines coming from similar regions are compared, one reasonably expects that the errors tend to partially cancel each other.

Adopting LTE, the line fluxes can be written in the form:

$$I_{10-4}(\mathrm{H}) = 2.00\,10^{-27} \exp(0.16/T_4) T^{-1.5} \int n(\mathrm{H}^+) n_e dV$$

$$I_{13-7}(\mathrm{He\,II}) = 1.00\,10^{-26} \exp(0.38/T_4) T^{-1.5} \int n(\mathrm{He}^{2+}) n_e dV$$

$$I_{10-9}(\mathrm{N\,V + O\,V}) = 2.36\,10^{-24} \exp(1.20/T_4) T^{-1.5} \int (n(\mathrm{N}^{5+}) + 1/2 n(\mathrm{O}^{5+})) n_e dV$$

$$I_{11-10}(\mathrm{O\,VI}) = 3.85\,10^{-24} \exp(1.30/T_4) T^{-1.5} \int n(\mathrm{O}^{6+}) n_e dV$$

$$I_{10-9}(\mathrm{C\,IV}) = 6.17\,10^{-25} \exp(0.75/T_4) T^{-1.5} \int n(\mathrm{C}^{4+}) n_e dV\,,$$

where all the quantities are expressed in cgs units and $T_4 = T_e/10{,}000$ K. From these, a rough estimate of the relative abundances can be obtained:

$$(n(\mathrm{N}^{5+}) + 1/2 n(\mathrm{O}^{5+}))/n(\mathrm{He}^{2+}) \simeq 0.01$$

$$n(\mathrm{O}^{6+})/(n(\mathrm{N}^{5+}) + 1/2 n(\mathrm{O}^{5+})) \simeq 0.6$$

$$n(\mathrm{He}^{2+})/n(\mathrm{H}^+) \simeq 0.02$$

the last relationship being very uncertain since lines arising from totally different regions are compared. Even with some uncertainty, however, the total $\mathrm{He}^+ + \mathrm{He}^{2+}$ abundance must be larger than 0.12, indicating an enrichment of He in the gas.

The observed upper limit for the C IV 10–9 (2.429 μm) line sets a strict constraint on the C^{4+} to $\mathrm{N}^{5+} + \mathrm{O}^{5+}$ abundance ratio:

$$n(\mathrm{C}^{4+})/(n(\mathrm{N}^{5+}) + 1/2 n(\mathrm{O}^{5+})) < 0.4\,.$$

The C^{4+} and N^{5+} ions are likely to be the most abundant ions of C and N in the highly ionized region close to the nova. On the other hand, O^{6+} is probably the most abundant oxygen ion, rather than O^{5+}. Therefore, whatever mixture of N and O abundances one assumes, the resulting C/(N + O) abundance ratio is at least a factor of two lower than solar. Also, if we assume that the O^{5+} is negligible compared to N^{5+}, the resulting C/N ratio (<0.4) is similar to that observed in some planetary nebula. This is exactly what one expects for material processed in the CNO cycle and it agrees very well with the current ideas about the nova outburst produced by non-equilibrium CNO burning near the white-dwarf surface.

III. Photometry

A) Visual photometry

Most of our photometric observations in the visual spectral range were carried out in the Walraven *VBLUW* photometric system with the 5 channel photometer attached to the Dutch 90 cm telescope at the European Southern Observatory. For a description of the instrument and the photometric system we refer to e.g. Rijf et al. (1969), and Lub and Pel (1977). Nova Mus 1983 was observed with this equipment during 27 nights between January 21 and February 25, 1983. An additional observation was carried out on March, 25, 1983. Observations in the Johnson *UBV* system were carried out by us on the 4 nights from January 24 to 28, with the standard *UBV* photometer attached to the Bochum 60 cm telescope at La Silla.

Figure 13 shows the *V*-lightcurve of Nova Mus from the date of its detection until the end of September. Our Walraven data have been transformed into Johnson *V*-magnitudes using the transformation formula by Lub and Pel. There is, however, a systematic difference of about 0.1 magnitudes between these transformed values and the Johnson *V* values measured by us, probably due to the strong emission lines of Nova Mus. Additional brightness values in our lightcurve are the visual estimates by Liller (1983) and Overbeek (1983), and photoelectric values by Nikoloff and Johnston (1983), Nikoloff et al. (1983), and Budding (1983). After February 25 visual magnitudes obtained by amateur astronomers of the Royal Astronomical Society New Zealand (RASNZ) and of the AAVSO have been used. If there was more than one measurement per night, an average value has been taken.

One can easily see that the visual estimates by Liller and Overbeck are systematically higher than the photoelectric measurements by about 0.5 mag. This overestimate of the *V* magnitude might be explained by the rather red colour of Nova Mus. The real *V* magnitude of the nova on the date of its detection (January 18.14) should have therefore been around 7.7 mag.

The lightcurve of Nova Mus 83 shows, after a steep decline during the first days, a slower decrease until about the end of April. There are daily variations of a few tenth of a magnitude and a brightness flare by mid of February. After a small increase in May the brightness of Nova Mus remained nearly constant for at least 5

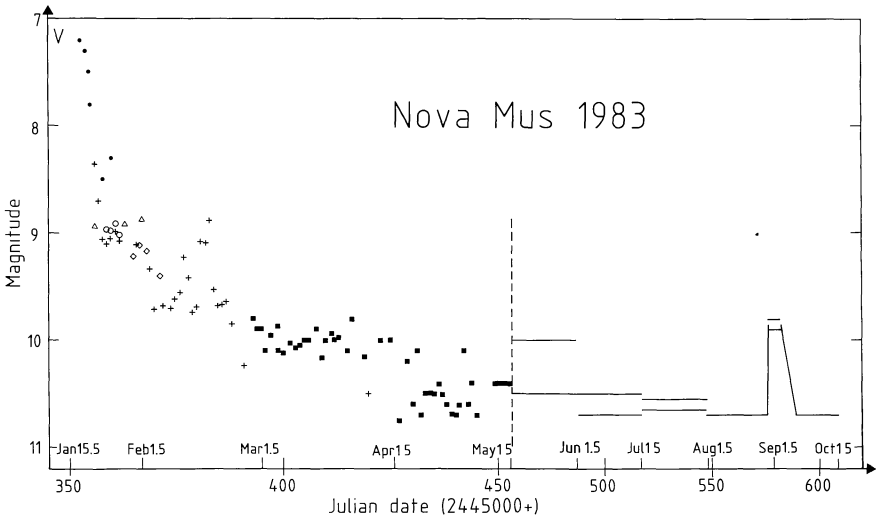

Fig. 13. Lightcurve of Nova Muscae 1983 until September 30, 1983. Please note the change of the scale after May 2 (right of vertical dashed line). From May 2 on only the upper and lower limits of the range of variability as given in the circulars of the variable star section of the RASNZ are indicated. Between August 1 and September 30, the brightness of the nova was rather constant at $V=10.6$ apart from the sudden increase around September 1. The individual symbols denote: ● Visual measurements (Liller, 1983; Overbeck, 1983), + Walraven photometry (this paper), ○ *UBV* measurements (this paper), □ *UBV* measurements (Nikoloff, 1983), △ *UBV* measurements (Budding, 1983), × Visual measurements (amateur astronomers of the RASNZ)

months at $V \approx 10.6$–10.7. Very remarkable is the brightening by about 1 mag around September 1. During one night (February 25) Nova Mus has been observed for 6 consecutive hours; no significant variations could be detected during that time.

B) Infrared photometry

Broad band infrared photometry in the *JHKLMN* bands was obtained with the ESO 3.6 m and 1 m telescopes. On the 1 m telescope the old Kreysa photometer (Kreysa, 1980) was used during the period January 21 to February 2. From February 7–10 the same telescope was equipped with the new ESO photometer (Moorwood, 1982). Both photometers were equipped with an InSb detector and measurements in the *J*, *H*, *K*, and *L* bands were carried out. On the 3.6 m telescope data were obtained in *JHKLM* with the standard photometer in the InSb mode on January 26, 31, and February 2, and in *KLMN* in the bolometer mode during January 27, 28, and February 1. The journal of our IR observations is given in Table 8. We would like to note that the *L* filters used at the 3.6 m and 1 m telescope differ slightly in central wavelength (3.8 μm and 3.6 μm respectively). The *L* filter centered at 3.8 micron contains the strong Brackett emission line at $\lambda = 4.05$ μm which contributes a considerable fraction to the total radiation. This may explain the higher brightness in the *L* band measured with the 3.6 m telescope.

Table 8. Magnitudes of Nova Muscae 1983. The statistical error is typically smaller then 0.05 mag. Only for those values for which we did not give a hundredth magnitude, the error is between 0.05 and 0.1 mag

Julian Date (2445300+)	Date (UT)		*J*	*H*	*K*	*L*	*La*	*M*	*N*
55.81	January	21.31	6.28	6.16	5.71		4.72		
56.77		22.27	6.41	6.38	5.87		4.77		
57.80		23.36	6.53	6.43	5.88		4.72		
58.81		24.31	6.45	6.41	5.83		4.67		
59.74		25.24	6.47	6.42	5.89		4.73		
60.75		26.25	6.43	6.38	5.81		4.66		
60.90		26.40		6.35	5.81	4.46		4.16	
61.75		27.25	6.47	6.50	5.97		4.80		
61.89		27.39			5.91	4.54		4.3	3.0
62.92		28.42			5.88	4.50		4.31	2.9
63.88		29.38	6.55	6.57	5.92		4.73		
64.89		30.39	6.52	6.54	5.95		4.77		
65.79		31.29	6.45	6.58	5.91		4.80		
65.87		31.37			5.86	4.52		4.3	
66.76	February	1.26	6.36	6.50	5.87		4.68		
66.83		1.33				4.35		4.03	2.9
67.77		2.27	6.44	6.62	5.92		4.74		
67.89		2.39		6.58		4.56		3.82	
72.88		7.38	6.28	7.16	6.53		5.14		
74.89		9.39	6.31	7.22	6.58		5.32		
75.87		10.37	6.33	6.98	6.27		5.11		

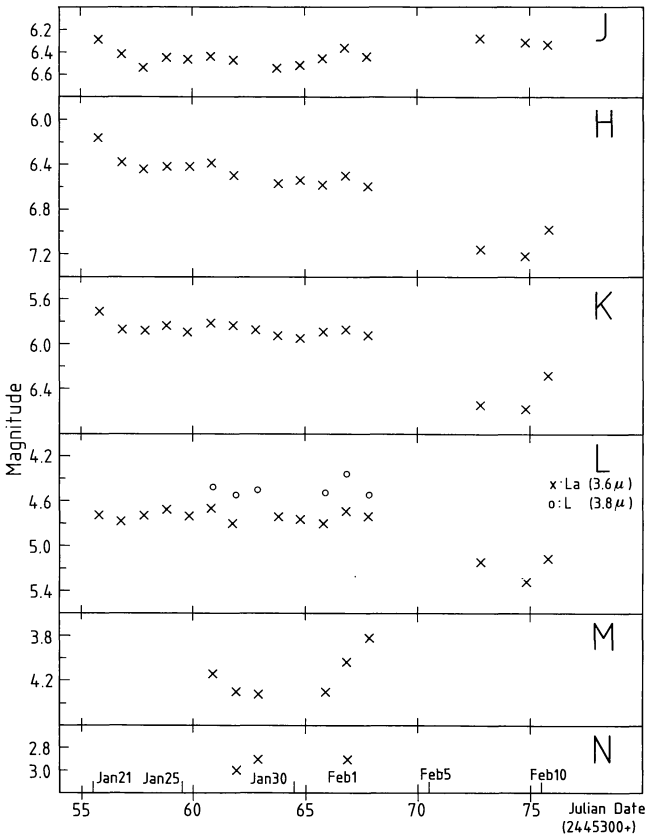

Fig. 14. Infrared lightcurves of Nova Muscae 1983

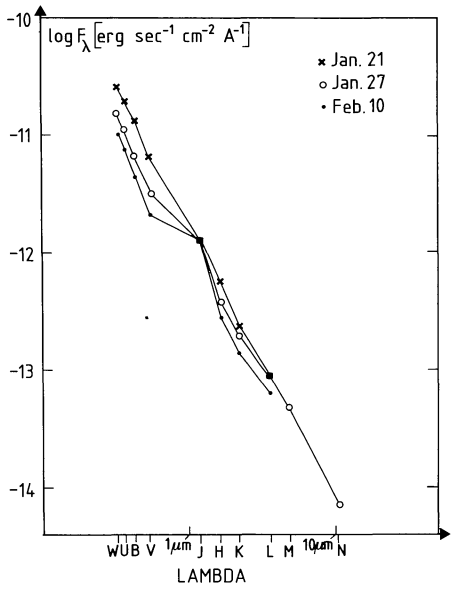

Fig. 15. Flux distributions of Nova Muscae 1983 at different epochs. For dereddening $E_{B-V}=0.45$ has been used

Infrared lightcurves measured in the *JHKLM* filters are presented in Fig. 14. During the first 13 days the behaviour in the *JHKL* filters is essentially the same: A slight decay from the first to the second night is followed by a longer period with constant brightness. After a gap of 4 days in the observations the brightness in *H*, *K*, and *L* had decreased by about 0.6 mag, whereas in the *J* band the brightness still remains constant. In the *M* band only 6 data points were measured. Here the flux increased by about 0.5 mag within 2 days (January 31 to February 2).

Additional IR observations were carried out during daytime on August 18.92 UT and 19.8 UT, 1983 using the InSb photometer attached to the ESO 1 m telescope. No significant variations were found between these two days. The mean magnitudes are: $J=8.35\pm0.02$, $H=9.66\pm0.07$, $K=8.62\pm0.04$, and $L=7.53\pm0.08$, and $M\geqq6.5$. Note the relative decrease by about one magnitude in the *H*-band.

C) Spectral energy distribution

Figure 15 shows the dereddened spectral energy distributions (SED) for several days between January 21 and February 10. For dereddening $E_{B-V}=0.45$ was used. Generally the flux increases from the infrared to the ultraviolet spectral range ($\lambda>3200$ Å) obeying a power law $F_\lambda\propto\lambda^{-\alpha}$ with $2\leqq\alpha\leqq2.3$. There is no obvious change in the slope of the SED from January 21 to February 10. The overall intensity dropped by about a factor 1.5 during this time intervall. The spectral index found here is characteristic of free-free emission of an optically thin gas.

Several comments should be made in this regard. Due to the strength of the emission lines the broad-band photometry fluxes are considerably influenced by line radiation. For instance, the two bright lines HeI 2.058 μm and Brackett gamma contribute about 50% to the *K* magnitude. Therefore, variations of the broad-band filter fluxes could be caused by line radiation instead of continuum variations. Also the opposite could be the case: a decreasing continuum flux could be compensated by an increasing flux of an emission line and hence the total broad band filter flux remains constant. This effect might explain the constant flux in the *J* band after February 3 while the flux in the other wavelength bands decreases. The HeI λ10830 line which might considerably contribute to the *J* flux (e.g. Whitelock, 1983) may have increased during this period as did HeI λ4471 in the visual spectral range between January 29 and February 20. However, since no spectrum in the visual spectral range between these two days is available, the exact date of the increase in the HeI line strength remains uncertain.

An increase of the flux in the *M* band giving rise to an excess on February 2, is a strong indication for the formation of the yet unidentified 5 micron feature found in several other novae during the free-free emission stage (e.g. Ney and Hatfield, 1978). Unfortunately no *M* band data are available after February 2. We would like to note that the time base of our IR observations is too short in order to establish a t^{-2} time dependence of the flux, the decay rate expected for an optically thin shell expanding at constant velocity and thickness (e.g. Ennis et al., 1977).

No formation of an optically thick dust shell has been observed by the end of September 1983. Indications of dust formation would have been a significant drop of the visual lightcurve or an increase of the IR flux. Neither was observed.

D) The prenova

Nova Muscae 1983 could be identified with a very faint object on the SRC *J* sky atlas. A finding chart is given in Fig. 16. An attempt has been made to measure the brightness of the prenova using the magnitude-image diameter calibration of the UKSTU *J*-survey plates given by King et al. (1981). Since this is a mean calibration

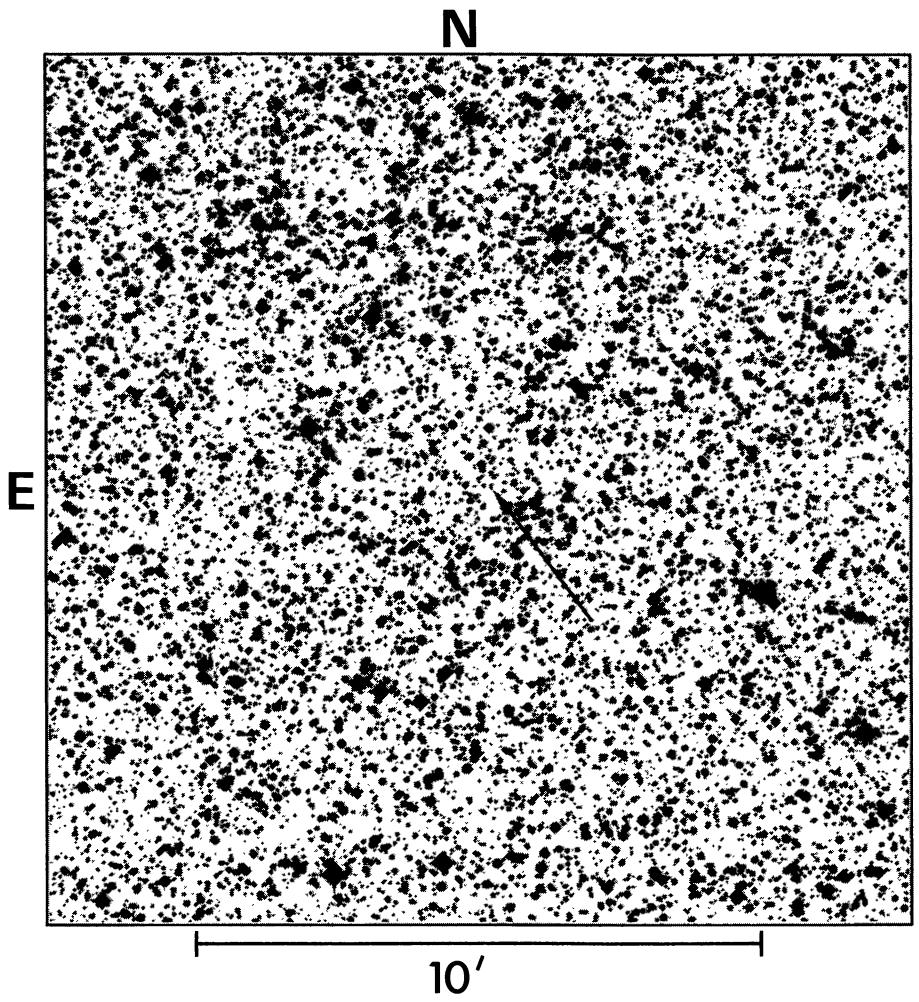

Fig. 16. Identification of the prenova and finding chart of Nova Muscae 1983 from a IIIaJ plate of the SRC sky survey

and therefore differs somewhat from plate to plate, the open cluster NGC 4052 (Engver, 1968) being in the same field No. 94 as Nova Mus 83 has been used as an independent calibration sequence. As a result we have found the calibration sequence to be 0.65 mag weaker for a given diameter than the mean calibration of King et al.

The diameter of Nova Mus 83 in its minimum state was measured as $D=50$ micron. There are, however, some problems by applying King et al.'s relation, since the faintest star used for construction of their calibration curve has a diameter of 60 micron yielding a magnitude $m_j=0.8B+0.2V=20.5$. By extrapolating the calibration curve and by applying the correction of 0.65 mag one obtains as j-magnitude of the prenova $m_j=23.0$. However, it is very uncertain whether the extrapolation of King et al.'s relation is valid for such small diameters. One would rather expect a considerable flattening of the calibration curve. Moreover, the magnitude limit of the SRC J-plates is about 23 mag or somewhat brighter. Since the prenova is clearly visible on the SRC plate as well as detectable on the corresponding ESO quick blue survey plate (which goes less deep than the SRC J-survey) it should be brighter than the extrapolated brightness. An upper brightness limit can be given by assuming the most extreme case of a totally flat extrapolation of the calibration curve. With the correction of 0.65 mag one obtains $m_j \geqq 21.15$. With $E_{B-V}=0.45$ and $(B-V)_0=0.0$ for a nova in minimum state one gets as upper limit for the visual magnitude $m_V \geqq 20.8$. On the other hand, since a totally flat extrapolation is not very probable, it is rather safe to assume that the visual brightness of the prenova is equal to or below 21st magnitude.

IV. Discussion

An attempt has been made to derive the distance of Nova Mus 1983 from the equivalent width of the interstellar lines. We determined the equivalent widths of the interstellar Ca II K line to be $W_K=0.43\pm0.02$ Å as the mean from five plates. Hobbs (1974) established a correlation between the distance d and W_K for approximately 80 galactic stars. Extrapolation of this relation to $W_K=0.43$ would yield $D=1.7\pm0.3$ kpc for Nova Mus 83. It is unlikely, however, that Hobbs' relation holds for $d>1$ kpc. Also, it depends on galactic latitude and longitude. The most comprehensive study yet of the distribution of interstellar matter as a function of distance has been carried out by Neckel and Klare (1980). They found that in the direction of Nova Mus 83 ($l\approx297°$, $b\approx-5°$) the total visual absorption A_V linearly depends on d for $d<1$ kpc, but stays constant at $A_V\approx1.2$ mag for $d\geqq1$ kpc out to about 5 kpc. Hence, the W_K vs. d relation is not valid for distances in excess of 1 kpc in this part of the sky and we regard the distance of 1 kpc as a lower limit only.

On the other hand, Neckel and Klare's relation provides a lower limit for the interstellar extinction of $E_{B-V}\geqq0.40$ mag. Their

$A_V(d)$ relation is rather well established up to a distance of about 2 kpc. At this distance the nova is already 175 pc away from the galactic plane, and we do not expect the section of the line of sight beyond this point to significantly contribute to the reddening of Nova Mus. Hence the interstellar extinction E_{B-V} should not exceed the lower limit 0.40 mag by a large amount in agreement with $E_{B-V}=0.45$ mag as derived from the 2200 Å feature in the ultraviolet.

Another approach to determining the distance is by estimating the absolute magnitude of Nova Mus. The absolute magnitude of a nova at maximum may be calculated from the luminosity-lifetime relation $M_V=-11.75+2.5\log t_3$ (Schmidt-Kaler, 1957) where t_3 is the time in days for the nova to decline from maximum to 3 magnitudes below the maximum. For Nova Mus 83 we are in the unlucky situation that we do not know whether the first detection was really at, or, at least very close to maximum. Our data provide evidence that Nova Mus was, in fact, discovered a few days past maximum:

a) Our first photometric and infrared observations were carried out on January 21, 3 days after discovery. The spectral energy distribution was that of an optically thin free-free emitter. However, general wisdom indicates that this is already the second stage in the evolution of a nova's SED which starts with blackbody radiation from an optically thick pseudophotosphere (e.g. Gallagher and Ney, 1976; Ney and Hatfield, 1978; Ennis et al., 1977; Wamsteker, 1980; Gehrz et al., 1980a, 1980b). Even for Nova Cyg 1975 (=V1500 Cyg), the fastest nova yet observed, Gallagher and Ney report the onset of the optically thin free-free radiation phase not earlier than 4.2 days after maximum. For the other investigated novae the free-free phase began even later; for the fast Nova Cyg 1978 about 8 days after eruption (Gehrz et al., 1980a), for the moderately fast Nova Ser 1978 6 days after eruption (Gehrz et al., 1980b), and for the also moderately fast Nova Vul 1976 (Ney and Hatfield) 8 days after eruption. It is therefore highly improbable that Nova Mus 1983 should have been in the optically thin free-free phase as early as 3 days after maximum.

It is therefore safe to assume that we first observed Nova Muscae 83 at least 5 days after maximum. Extrapolating the visual lightcurve towards this earlier date with the mean decline rate of the first 4 (observed) days, 0.25 mag/day, we find a maximum brightness V_{max} of $\lesssim 7.3$ mag.

b) Our first spectrum was also taken 3 days after discovery on January 21 at $V=8.3$ mag. The very pronounced diffuse enhanced character and the presence of the 4640 Å emission feature qualitatively show that the nova had already undergone some evolution. According to Payne-Gaposchkin (1957), the earliest appearance of the diffuse enhanced spectrum occurs at 0.7 mag below maximum brightness and 4 days after the outburst for fast novae, and at 2.3 mag below maximum brightness and 16 days after outburst for slow novae, respectively.

On the other hand, the diffuse enhanced spectrum disappears 3.0 mag below maximum brightness. There is considerable evidence that this happened when the V magnitude faded from 9.8 to 10.1 mag between February 22 and 25. The strength of the dea components decreased considerably from the Coudé spectra of February 21 to 24 (cf. Fig. 1). In addition, there is no evidence for any dea (and pa) absorption feature in the UV spectra taken 10 days later on March 4.

The first NIII absorption feature (λ4097) was found when the nova was at $V=9.1$. The first appearance of this feature for fast novae should occur at 2.3 mag below the maximum (Payne-Gaposchkin, 1957).

Hence, from the appearance and disappearance of spectral features the most probable maximum brightness seems to have been $V_{max}\approx 7.0$ mag. The extrapolation of the V-lightcurve with the mean decline rate for the first days (see above) then suggests that the outburst occurred about on January 14–15, 1983, 3 to 4 days before the discovery. From this we get as most probable lifetime $t_3\approx 40$ days. However, if the nova was as bright as 6.7 mag at maximum (which cannot be fully excluded) decay by 3 mag would have been reached on February 4, and t_3 would be as short as 22 days.

We therefore classify Nova Mus 83 as a moderately fast to fast nova according to Payne-Gaposchkin's classification scheme. Several other properties found from our data support this classification:

1) The lower limit of the outburst amplitude is about 14 magnitudes. This is one of the largest outburst ranges ever observed (e.g. Payne-Gaposchkin, 1977). Since there is a correlation between speed class and outburst amplitude in the sense that faster novae have larger outburst ranges, the large amplitude favours the classification as a fast nova.

2) There exists a general correlation between speed class and expansion velocity (Payne-Gaposchkin, McLaughlin, 1960). According to this classification Nova Mus 83 is undoubtedly a fast nova.

3) Slow novae stay in the diffuse enhanced stage only during a narrow brightness interval of $\Delta m=0.3$ mag. (Payne-Gaposchkin, 1957), whereas Nova Mus remained in the diffuse enhanced stage for $\Delta m\simeq 1.7$ mag. This obviously argues against its classification as a slow nova.

For the first four months Nova Mus displayed a rather normal lightcurve for a certain type of fast nova: steep decrease, followed by a slower decrease with oscillations. The following period during which Nova Mus irregularly oscillated around a constant mean brightness level for at least 5 months is, however, rather uncommon. The only nova known to have shown a similar behaviour is DN Gem (=Nova Gem 1912). This nova which had a similar lifetime of $t_3=46$ days also remained for several months at a constant brightness level about 3.5–4 mag below the maximum brightness (Payne-Gaposchkin, 1957). Another similarity between Nova Mus and DN Gem are the radial velocities of the absorption systems. The radial velocities of the pa and dea systems of Nova Mus agree well with those of absorption II and III of DN Gem according to Payne-Gaposchkin' classification. The outburst range of DN Gem, however, is only 11.5 mag, and hence much smaller than that of Nova Mus.

It is now possible to obtain a rough estimate of the distance D to Nova Muscae 83. With our preferred value of $t_3=40$ days we get $M_V=-7.75$. Assuming $V_{max}=7.0$ and $A_V=1.35$ we obtain $D=4.8$ kpc. Taking into account the uncertainties in the various quantities we estimate the error in the distance to about ± 1 kpc.

Using this distance we derived a lower limit to the luminosity from the SEDs of January 21 and February 10 (see Fig. 15). For wavelengths longer than the IR regime we assume that the flux distribution may be extrapolated as $F_\lambda\propto\lambda^{-2}$. For the UV spectral range shortward of 3200 Å we cannot make a safe assumption on the flux distribution, since our earliest IUE spectrum was taken on February 18. For January 21 integration of the flux distribution for $\lambda\geqq 3200$ Å yields a lower limit to the luminosity $L\geqq 3.8\,10^4 L_\odot$, i.e. equal to the Eddington luminosity L_{Edd} for a $1\,M_\odot$ white dwarf. If the flux distribution decreased in the UV as it did for Nova Sgr 1982 early in the decline (Wargau et al., 1983) the total luminosity would be around $1.5\,L_{Edd}$. This is consistent with thermonuclear

runaway theories of nova outbursts. According to e.g. Sparks et al. (1978) and Starrfield et al. (1978) the achievement of a luminosity at maximum light close to L_{Edd} is one of the main features of the thermonuclear runaway.

On February 10, the luminosity longward of 3200 Å is $L=0.4L_{Edd}$. Still our earliest IUE spectrum was taken 8 days later. If we take that spectral distribution as representative also of February 10, the total luminosity is $L=0.9L_{Edd}$. Finally, for March 4 the short-wavelength IUE spectrum and the visual magnitude of 10.0 mag permit a rough estimate of the luminosity if the assumption is made that $F_\lambda \propto \lambda^{-2}$ still holds for the optical and IR range. The resulting total luminosity is $L=0.5L_{Edd}$.

For the subsequent time interval of 3 weeks we find that the corresponding lower limits (based on visual and infrared photometric data) to the luminosity decrease. This does not contradict, however, the concept of a constant bolometric luminosity during that phase. With increasing time elapsed from outburst the temperature of the expanding optically thin shell increases and hence the relative amount of the free-free emission emitted in the ultraviolet spectral region is expected to increase (Stickland et al., 1980).

V. Conclusions

Spectroscopic and photometric observations of Nova Mus 1983 were carried out during its early decline phase over a wide spectral range from 1200 Å to 10 μm. Our main conclusions are:

Nova Mus 83 was a moderately fast to fast nova which was discovered several days after its maximum brightness. The most probable maximum brightness and lifetime t_3 are $V \approx 7$ mag and $t_3 \approx 40$ days, respectively. With the interstellar extinction $E_{B-V}=0.45$ mag a distance of $D=4.8\pm1$ kpc has been derived. The lightcurve of Nova Mus, with its long stay around a constant mean brightness, is rather unusual for a fast nova.

The prenova can be identified with a very faint object of $V \geqq 21$ mag. The outburst range is therefore $\Delta m \geqq 14$ mag which is one of the largest outburst ranges ever observed for novae.

The line profiles of the emission lines display a complex structure: several emission components, broad wings, and several absorption systems are present. Indications are found that the line profiles depend on the ionization state. From this one may conclude that the ejection of the envelope was highly asymmetric. The envelope seems to have a very complex structure and geometry with rather different excitation conditions for different regions. The simultaneous appearance of lines of highly ionized species as Nv, Ov, etc., neutral lines, and molecular bands in the infrared and ultraviolet spectra clearly shows that regions of very different temperatures existed simultaneously in the shell.

The molecular lines indicate the presence of molecules associated with dust in the surroundings of Nova Mus. This material may be either in the outer cooler regions of the expanding envelope, or, alternately, material which was deposited in the circumstellar region by the stellar wind which has been active during the minimum phase.

A possible overabundance of He/H as compared to solar values is indicated. The N/C and N/O ratios show a strong overabundance of nitrogen with respect to solar C and O abundances. From the strength of the CNO lines one may also suspect an overabundance of these elements to hydrogen as compared to solar values. This is entirely consistent with the thermonuclear runaway model of nova outbursts with hydrogen being burnt via the CNO cycle. This conclusion is also supported by the luminosity of Nova Mus 83 after outburst which was of the order of the Eddington luminosity of a white dwarf of one solar mass.

Acknowledgements. We would like to thank the staff of the European Southern Observatory on Cerro La Silla, Chile and of the ESA Villafranca Satellite Station for their help during the observations. We are especially indebted to Dr. F. Bateson and his amateur astronomers of the RASNZ who informed us about the nova outburst and who provided us with most of the visual observational data. We acknowledge the AAVSO data sent to us by Dr. J. Mattei. We are grateful to Dr. O. Stahl (LSW Heidelberg) for carrying out some of the IR observations and his help with the reduction and to Dr. J. Cuypers (Leuven) for carrying out some Walraven photometry. We thank Dr. R. Williams (ESO) for critically reading the manuscript and Drs. H. Ritter (MPA, Garching), M. Friedjung (Paris), and A. Cassatella (ESA) for valuable discussions. We wish to thank for the permission of the MPIA (Heidelberg) to use their Grant measuring machine. C.L., G.K., and B.W. were supported by the Deutsche Forschungsgemeinschaft (SFB 132 A).

References

Aitken, D.K., Roche, P.F., Allen, D.A.: 1982, *Monthly Notices Roy. Astron. Soc.* **200**, 69P
Allamandola, L.J., Greenberg, J.M., Norman, C.A.: 1979, *Astron. Astrophys.* **77**, 66
Allen, D.A., Baines, D.W.T., Blades, J.C., Whittet, D.C.B.: 1982, *Monthly Notices Roy. Astron. Soc.* **199**, 1017
Avni, Y.: 1976, *Astrophys. J.* **210**, 642
Baldwin, J.A., Netzer, H.: 1978, *Astrophys. J.* **226**, 1
Blades, J.C., Whittet, D.C.B.: 1980, *Monthly Notices Roy. Astron. Soc.* **191**, 701
Budding, E.: 1983, *IAU Circ.* **3853**
Burgess, A., Seaton, M.J.: 1960, *Monthly Notices Roy. Astron. Soc.* **121**, 471
Duerbeck, H.W., Wolf, B.: 1977, *Astron. Astrophys. Suppl.* **29**, 297
Engver, N.: 1968, *Arkiv Astron.* **4**, 53
Ennis, D., Becklin, E.E., Beckwith, S., Elias, J., Gatley, I., Matthews, K., Neugebauer, G., Willner, S.P.: 1977, *Astrophys. J.* **214**, 478
Felli, M., Oliva, E., Natta, A., Stanga, R., Beckwith, S.: 1982, in *Galactic and Extragalactic Infrared Spectroscopy, XVIth ESLAB Symp.* p. 13
Ferland, G.J., Lambert, D.L., Netzer, H., Hall, D.N.B., Ridgway, S.T.: 1979, *Astrophys. J.* **227**, 489
Gallagher, J.S., Ney, E.P.: 1976, *Astrophys. J. Letters* **204**, L35
Gehrz, R.D., Hackwell, J.A., Grasdalen, G.L., Ney, E.P., Neugebauer, G., Sellgren, K.: 1980a, *Astrophys. J.* **239**, 570
Gehrz, R.D., Grasdalen, G.L., Hackwell, J.A., Ney, E.P.: 1980b, *Astrophys. J.* **237**, 855
Goebel, J.H., Bregman, J.D., Witteborn, F.C., Taylor, B.J., Willner, S.P.: 1981, *Astrophys. J.* **246**, 455
Grasdalen, G.L., Joyce, R.R.: 1976, *Nature* **259**, 187
Hobbs, L.M.: 1974, *Astrophys. J.* **191**, 381
King, D.J., Birch, C.J., Johnson, C., Taylor, K.N.R.: 1981, *Publ. Astron. Soc. Pacific* **93**, 385
Krautter, J., Klare, G., Wolf, B., Duerbeck, H.W., Rahe, J., Vogt, N., Wargau, W.: 1981, *Astron. Astrophys.* **102**, 337

Kreysa, E.: 1980, Ph. D. Thesis, Univ. Bonn
Liller, W.: 1983a, *IAU Circ.* **3764**
Liller, W.: 1983b, *IAU Circ.* **3768**
Lub, J., Pel, J.W.: 1977, *Astron. Astrophys.* **54**, 137
McLaughlin, D.B.: 1960, in *Stars and Stellar Systems*, Vol. VI, ed. J. L. Greenstein, Chicago Univ. Chicago Press, p. 585
Moorwood, A.F.M.: 1982, *The Messenger* No. **27**, 11
Neckel, Th., Klare, G.: 1980, *Astron. Astrophys. Suppl.* **42**, 251
Ney, E.P., Hatfield, B.F.: 1978, *Astrophys. J. Letters* **219**, L111
Nikoloff, I., Johnston, J.: 1983, *IAU Circ.* **3766**
Nikoloff, I., Birch, P., Harwood, D.: 1983, *IAU Circ.* **3771**
Overbeek, M.D.: 1983, *IAU Circ.* **3764**
Osterbrock, D.E.: 1974, Astrophysics of Gaseous Nebulae, Freemann, San Francisco
Payne-Gaposchkin, C., 1957: The Galactic Novae, North-Holland, Amsterdam
Payne-Gaposchkin, C.: 1977, in *Novae and Related Stars*, ed. M. Friedjung, p. 3
Rijf, R., Tinbergen, J., Walraven, Th.: 1969, *Bull. Astron. Inst. Netherlands* **20**, 279
Schmidt-Kaler, Th: 1957, *Z. Astrophys.* **41**, 182
Sparks, W.M., Starrfield, S., Truran, J.W.: 1978, *Astrophys. J.* **220**, 1063
Starrfield, S., Truran, J.W., Sparks, W.M.: 1978, *Astrophys. J.* **226**, 186
Stickland, D.J., Penn, C.J., Seaton, M.J., Snijders, M.A.J., Storey, P.J.: 1981, *Monthly Notices Roy. Astron. Soc.* **197**, 107
Struve, O., Wurm, K.: 1938, *Astrophys. J.* **88**, 84
Wamsteker, W.: 1979, *Astron. Astrophys.* **76**, 226
Wargau, W.: 1984 (in preparation)
Wargau, W., Drechsel, H., Rahe, J.: 1983, in *Proc. IAU Coll.* **80**, Lembang (to appear)
Whitelock, P.A.: 1983, *IAU Circ.* **3771**
Williams, R.E.: 1982, *Astrophys. J.* **261**, 170
Williams, R.E.: 1983 (private communication)
Williams, R.E., Woolf, N.J., Hege, E.K., Moore, R.L., Kopriva, D.A.: 1978, *Astrophys. J.* **224**, 171
Williams, R.E., Sparks, W.M., Gallagher, J.S., Ney, E.P., Starrfield, S.G., Truran, J.W.: 1981, *Astrophys. J.* **251**, 221